HARD-FACING WITH ELECTRO-SPARK DEPOSITION

DOE/RL/10308--1

DE84 001502

By

KENNETH PAUL KEES

A thesis submitted in partial fulfillment of
the requirements for the degree of

MASTER OF SCIENCE

WASHINGTON STATE UNIVERSITY
College of Engineering

1983

DISCLAIMER

To the faculty of Washington State University :

The members of the Committee appointed to

examine the thesis of KENNETH PAUL KEES

find it satisfactory and recommend that it be accepted.

Gary L. Sheldon
Chair

Jack T. Kimbrell

L. Hilden Kindall

AKNOWLEDGEMENT

I wish to extend a sincere thank-you and appreciation to my mentor and colleague Dr.Gary Sheldon, whose perseverence and direction brought this thesis from an idea to a reality. The interest, suggestions and support of Roger Johnson at HEDL and Professor Jack Kimbrell and Dr.Alden Kendall at WSU were of great help, and I thank you all.

HARD-FACING WITH ELECTRO-SPARK DEPOSITION

ABSTRACT

by Kenneth Paul Kees, M.S.
Washington State University, 1983

Chair: Gary L.Sheldon

A common method to improve wear resistance of metals in rubbing contact is to increase their surface hardness. Electro-Spark Deposition is a process which uses capacitive discharge pulses of high current passing through a hard carbide electrode in contact with and scanning the metal surface to be hardened. The result is a thin, hard, adherent coating of carbide deposited with a minimum of heat influence on the substrate and a significant increase in wear life of the coated metal.

Electro-Spark Deposition is similar to a micro-welding process. It is a simple, portable and inexpensive coating method, which has great potential for commercial utilization. This thesis is an in depth study of the parameters associated with the ESD process and the wear resistance of the coatings.

Table of Contents

List of Tables

List of Illustrations

1 INTRODUCTION

The Industrial Age brought widespread use of machinery to increase productive output. Today the tight constraints of economy demand the most efficient use of machines. A detriment to efficiency is wear of the metal of which the machine is made. This thesis consists of an investigation into a process to minimize wear.

Wear occurs in different forms. Fatigue and shock failure are extreme forms of wear. Corrosion and pitting take their toll under adverse environments and stresses. The most common type encountered is rubbing wear. Rubbing wear can be divided into two distinct types: adhesive and abrasive. Adhesion is a wear process in which the asperities of contacting metals fuse and pull one another loose from the base. This is especially evident in rubbing unlubricated similar metals together. Abrasive wear occurs after hard asperities are knocked loose and work between the contacting surfaces to cause breakdown. Rubbing wear is minimized by increasing the surface hardness of the metal, which increases its resistance to adhesion and abrasion (1).

Processes that increase the hardness of metals are many, each with its own advantages and limitations. Some processes include heat treating the base metal by quenching or second phase precipitation. Additional hardness at the surface can be obtained by flame, induction, case, nitride, anodize or work hardening. Finally, a hard coating may be applied to the surface by plating, hardfacing, vacuum deposition, plasma arc spraying, sputtering, or ESD (Electro-Spark Deposition). In the ESD process, an electrode of hard

material is rubbed across the surface of a base metal. A high positive current is pulsed rapidly through the electrode and grounded substrate, resulting in a short but intense melting of both materials. Some mixing occurs at the interface, after which the relatively large thermal mass of the substrate rapidly quenches the melt and a hard, amorphous coating is formed. Part of the electrode transfer is by discharge across the interstitial gap between the contacting metals, which is evidenced by the bright sparking that occurs during the process, hence the name Electro-Spark Deposition. The resulting coating is very hard and has a fine matte appearance. ESD dramatically increases the wear resistance of metals, yet is relatively simple and inexpensive to apply. It employs lightweight, portable apparatus and requires only a power supply as support equipment. Other advantages of the process include negligible heating and its subsequent effects on the substrate and a capability of depositing or coating any solid metal.

The investigation into ESD by Dr.Gary Sheldon at WSU and Roger Johnson at the Hanford Energy Development Lab (HEDL) over the past several years has evolved into a collaborative effort. A research grant was given by the Department of Energy through HEDL to WSU for developing a particular commercial application of ESD. The housings for fuel rods in a nuclear reactor core are subject to galling when being removed for fuel replacement and are also wear prone when banded together because of thermal expansion and contraction moving the ducts against one another. The high replacement cost of the ducts and the possibility of their becoming jammed in the core or damaged during removal makes a wear resistant coating necessary.

2 HISTORY OF ESD

The origins of ESD can be traced from 1924 when H.S.Rawdon observed that spark discharge between iron contact points caused a hardening of the iron surface. Rawdon surmised that the high local surface temperatures and rapid quenching by the cool contact mass caused a martensitic transformation in the iron, increasing its hardness. This he confirmed by further experimentation with copper and nickel contacts, neither of which showed increased hardness. No deposition occurred, merely a local heat treatment of the iron (2).

Further research into this phenomenon was not well recorded until the 1950's. In 1957, N.C.Welsh demonstrated that non-ferrous metals could be hardened if sparked in a suitable environment. By sparking titanium in an oil bath, Welsh formed titanium carbides in a reaction between the carbon in the oil and the titanium surface, yielding a durable layer on a material formerly prone to galling. He also found that steel surfaces showed increased spark hardness because of compounding with atmospheric oxygen and nitrogen (3).

It was also during the 1950's that publications released from the USSR indicated not only a familiarity with spark hardening, but that it was a process in commercial use. They reported the first use of hard carbide electrodes to deposit a coating on a base metal. This coating exhibited much greater wear resistance than the spark hardening by rapid quenching alone could produce (4)(5).

Both the hardening and deposition are conventionally done by vibrating an electrode against the workpiece in a make/break contact motion, discharging a capacitor and sending a large pulse of current through the electrode. Other schemes have been developed to increase deposition and improve surface finish, but are not in wide use (4)(6)(11)(12).

Applications in commercial use include hardening of metal cutting tools such as drills, milling cutters, saw blades, lathe tools and punching dies, as well as high wear machine components such as cams, axles, tappets and turbine blades. The wear life of these treated components increases by at least thirty percent, with some HSS cutting tools increasing useful life as much as four times. The commercial utilization of ESD in the United States is virtually nil, and available equipment is mostly experimental and not suitable for industrial use (6)(7)(8).

3 COATING CRITERIA

3.1 Wear Coefficient

In developing criteria for coatings to be applied to stainless ducts in a nuclear reactor, several constraints must be satisfied. To ensure that the constraints are met, the criteria must be testable and verifiable.

The most important constraint is that the coating must exhibit high resistance to wear. This resistance can be expressed as a factor "K", the wear coefficient, which appears in a basic wear equation derived by R.Holm in 1946 and confirmed by J.F.Archard in 1953 (9)(14):

$$W = K L d / H \qquad (3.1)$$

where,

W : volume loss from wearing surface

K : wear coefficient

L : normal force exerted on the wearing surface

d : distance of sliding over the wearing surface

H : penetration hardness of the wearing surface

The equation justifies increasing the surface hardness, as is commonly done to reduce wear, but also indicates that the wear coefficient plays an important role as well. The wear coefficient is characteristic not only of a particular material, but also the conditions under which the coating is applied. The four variables W, L, d and H are measurable quantities from which the wear coefficient may be determined. Minimum wear will occur when

K is small and H is large.

One method of determining "K" is to measure the friction coefficient "f" of the coated surface. An empirical equation using this method is (10):

$$\log K = 5 \log f - 2.27 \qquad (3.2)$$

This equation is not highly accurate, due to the nature of wear being difficult to quantify, but the relationships have proven themselves to be valid within a factor of two for many cases of adhesive and abrasive wear. Strict attention and care must be taken in evaluating the variables and depositing a consistent coating if scatter in data is to be minimized.

3.2 Nuclear Compatibility and Corrosion Resistance

Coatings used in the reactor should not be neutron absorbers and must be able to withstand a hot, corrosive, liquid sodium environment. Resistance to radiation also needs evaluation.

3.3 Surface Characteristics

An esthetic requirement for the final coating is that it should be pleasing to the eye. Burn marks, streaks and uneveness tend to detract from the quality of the finished product. When properly applied, ESD coatings have a uniform, fine matte appearance. Microscopic appearance should show a uniform covering of the substrate and a minimum of surface cracking.

The deposited coating should be as smooth as possible to minimize the wear coefficient (10). The tendency of ESD to deposit a very thin coating precludes building up a surface layer of sufficient thickness to permit grinding to a smooth finish. However, a light sanding of the coated surface to remove the highest asperities greatly enhances the wear coefficient and reduces the amount of adhesive and abrasive wear. Generally a final cover pass with a low power setting will both improve the surface appearance and minimize the roughness of the final coating.

Adherence of the coating is important in any kind of rubbing wear. Spalling from the substrate can result in a rapid de-scaling of the coating and in the least will contribute material for abrasive wear. The bond strength of the coating is a good indicator of the resistance to spalling, and can be measured according to the procedure outlined in Section 8.

Cracks in the coating are the result of thermal stresses that develop during quenching and contraction, similar to cracks which can occur in weld zones. Minimizing cracking will help to minimize spalling. Vertical cracks are less apt to spall than cracks parallel to the substrate. Cracks which form in ESD coatings tend to be vertical to the substrate.

4 ELECTRODES

4.1 Desired Qualities

Any conductive material can be used as an electrode in the ESD process. For maximum wear resistance, a very hard electrode is used, the hardest being sintered carbide. Commercial metal cutting grades of tungsten carbide using cobalt or nickel binders with tantalum and titanium carbide sometimes added are the most common source of electrode materials. Other hard refractories such as nitrides and borides have been used, but tend to be less durable than the carbides because of greater thermal fatigue at high temperatures.

4.2 Composition

The commercial grade carbide used in this research is CA-815 (chrome carbide), made by Carmet Carbide Company (32). Two special grades custom made by Carmet were R-241 (tungsten carbide) and R-242 (chrome carbide). These carbides all use nickel as a binder. Another carbide with a cobalt binder, GE 320, was also tested.

Non-carbide, high wear and corrosion resistant electrodes are available in commercial form. Those tested were Tribaloy 700 (nickel base) and Stellite 6 (cobalt base), supplied by the Cabot Corporation (33). The Stellite 6 and GE 320 cannot be used for reactor coatings because of neutron absorption by cobalt, but were tested for use as a data base for comparison with other electrode materials.

Some elemental electrodes were tested for the possibility of hard intermetallic compounds being formed as a result of electrode, substrate and atmosphere interactions. The electrodes included molybdenum, niobium and tantalum. Table 4.1 is a list of electrode compositions and properties.

4.3 Dimensions

Electrode sizes ranged from 3.175-5.00 mm (1/8-3/16 in) OD for the solid and 6.35 mm (1/4 in) OD with a 1.9 mm (1/16 in) wall thickness for the hollow electrodes, all of which were 25 mm (1 in) long.

The overhang of the electrode beyond the holder cannot be too great because it is relatively slender and brittle. Sticking from microwelds occuring at the contact interface results in a torque on the electrode sufficient for fracture if too much electrode is protruding. It is best if the electrode does not overhang the holder by more than six diameters.

Since the erosion rate of the electrodes is small, the relatively short allowable free length does not seriously affect the production capability because of the long replacement intervals. The time to erode a solid 3.175 mm (1/8 in) diameter R-242 electrode to half its 25 mm (1 in) length is 1.5 hours at moderately high power levels (130 watts) and typically covers 0.186 square meters (2 square feet).

TABLE 4.1

Composition and Properties of the Electrodes

Electrodes		Elements	%	Density	Melting Point	
Carbides:						
R-241	Tungsten	WC	79	12.5 g/cc	1453 C	*
		TiC	12			
		TaC	4			
		Ni	5			
R-242	Chromium	CrC	80	6.45	1453	*
		Cr2C3				
		TiC	10			
		Ni	10			
CA-815	Chromium	CrC	85	6.97	1453	*
		CrC3				
		Ni	15			
GE-320	Tungsten	WC	64	9.7	1495	*
		TiC	25			
		TaC	5			
		Co	6			
Non-Carbide:						
T-700		Ni	50	9.0	1590	
		Mo	32			
		Cr	15			
		Si	3			
Stellite		Cr	28	8.17		
		C	1			
		W	4			
		Co	67			
Elemental:						
		Molybdenum		10.22	2617	
		Tantalum		16.65	3880	
		Niobium		8.57	2468	

* - melting point of binder

5 PULSE GENERATION AND CONTROL

5.1 Interrupted Electrode Contact

The basic spark generation and control circuit shown in Fig 5.1 has remained relatively unchanged since its inception in the 1950's (13). N.C.Welsh and C.S.Kahlon have used similar circuits in their research (7)(15). The electrode is mounted on a spring return solenoid which vibrates at a fixed 100 hz frequency (using 50 hz European AC power), making and breaking contact between the electrode and work surface. At make, the energy stored in the capacitor begins to discharge through the electrode and grounded workpiece, and continues to flow between them at break as a spark discharge.

The resistor which charges the capacitor functions to limit the spark duration and the gap distance over which the spark will be continuous. There is an optimum gap distance for maximum transfer efficiency (4), after which the workpiece weight gain per unit of energy does not increase with voltage (15), and hence there is an optimum value of resistance (16).

The maximum energy dissipated in one pulse is the energy stored in the capacitor:

$$E = 1/2\ C\ V^{**}2 \qquad (5.1)$$

E : energy in joules

C : capacitance in farads

V : volts across the capacitor

Total power is determined from the frequency of pulses for a given energy per pulse:

$$\text{Power} = (\text{Joules/Pulse})*(\text{Pulses/Second}) \qquad (5.2)$$

Since the pulse frequency is fixed by the solenoid cycle, power is controlled by adjusting the pulse energy. Changing the voltage will upset the optimum gap distance, leaving capacitance as the favored adjustable parameter. Capacitors range in size between 10 and 1000 micro-farads, while the voltages are fixed at one or two values between 20 and 120 volts (6)(15).

The deposited weight increases with energy (capacitance), but not linearly over a wide range (15). The wear resistance of the coating does not increase continuously with the weight deposited, but passes through a maximum (16), indicating the existence of an optimum value of capacitance (energy).

There are other circuits being used now which superimpose a higher frequency pulse on the electrode to increase power, as well as other types of applicators which use continuous contact electrodes, but the details of the control and generation of the pulse are not well described in literature (11)(13).

5.2 Continuous Electrode Contact

The spark control circuit for continuous contact electrodes used in ESD research at WSU is shown in Fig 5.2. The pulse frequency is controlled by a variable clock pulse at the gate of the SCR (Silicon Control Rectifier) through which the capacitor discharges. Because the gap is fixed and small, it is possible to use a voltage as well as a capacitive control of spark energy. Voltages up to 220 volts can be used before the transfer efficiency begins to decrease.

The advantage of voltage control is twofold: one, the squared relation of voltage to energy requires only small changes of voltage to give a wide range of energy and two, a variable transformer has a continuous range of adjustment, is more convenient to adjust than a bank of capacitors and can be metered easily.

The size of capacitors used in the sparking circuit range between 10 and 200 micro-farad. The voltage is adjustable from 0 and 250 Volts and the pulse frequency is stepped between 500 and 1500 Hertz. The maximum energy and power available are 6.25 Joules and 9375 Watts.

An important parameter to be controlled is the pulse duration. The discharge period is a function of the capacitance, resistance and inductance in the discharge path. If the resistance of the discharge path is less than the value for critical damping, the discharge will oscillate. The pulse duration is shorter for an underdamped than an overdamped discharge, and is a function only of (LC)**1/2, the resonant period of the system.

Underdamped oscillation will overshoot the zero voltage level and cause a reversal of current. Current reversal at the electrode is prevented by a blocking diode in the discharge path.

By using low resistance power leads and minimizing resistance at electrical junctions, the pulse can be made to oscillate. Once oscillation occurs, the pulse period can be further decreased by using low inductance power leads and decreasing the discharge capacitance. The discharge capacitor has a limited size reduction, because the voltage must be increased to maintain equivalent energy levels and will eventually exceed the value beyond which transfer efficiency begins to decrease. Another limiting factor for short duration pulses is the switching time of the SCR. The pulse shapes and durations for increasing values of discharge capacitance are shown in Fig 5.3. The pulses are seen to be underdamped with a single overshoot and to have progressively longer durations.

A short duration pulse works well with continuous contact electrodes, allowing a rapid mass transfer rate and less tendency for lumping, a phenomenon described in Section 6. The operating range that seems to work best for high deposition and low lumping is 175-200 volts across a 5-25 micro-farad discharge capacitor with a pulse duration of 5-10 micro-seconds.

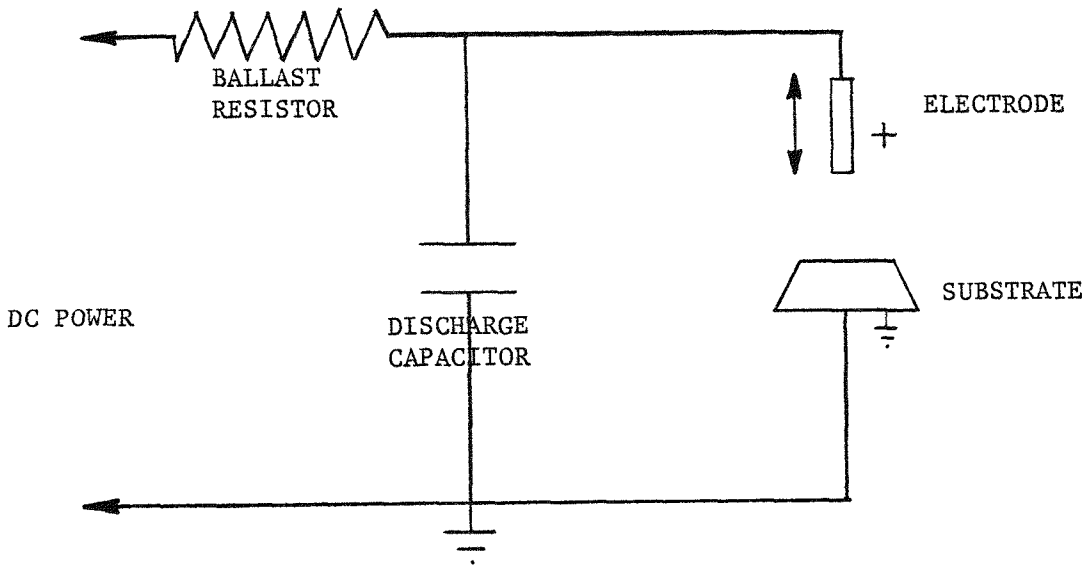

Fig 5.1--Pulse Circuit Diagram For the Interrupted Contact Electrode

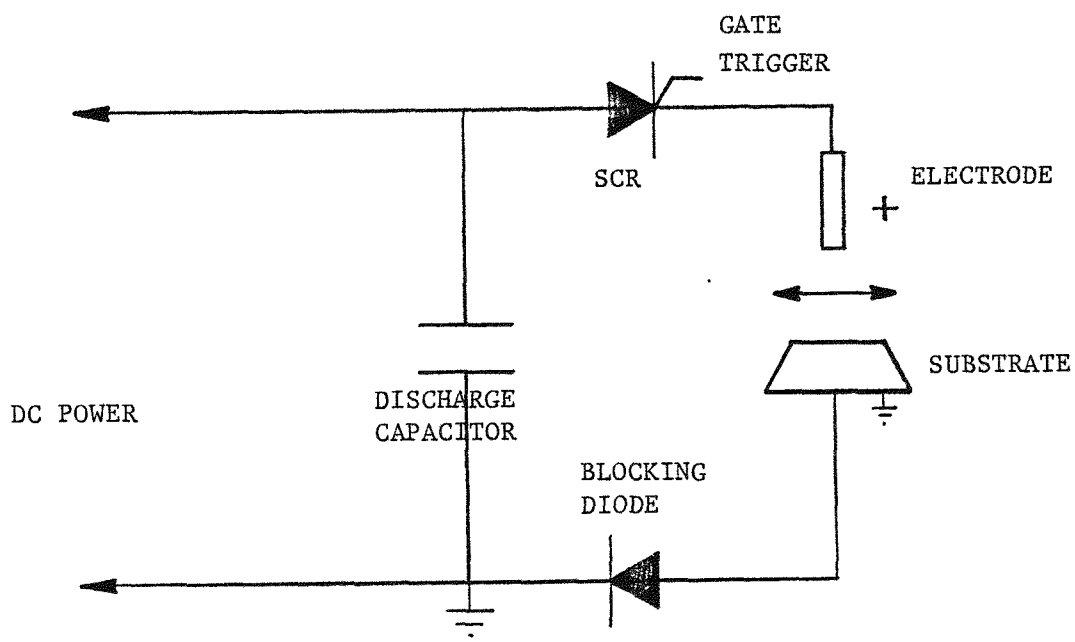

Fig 5.2--Pulse Circuit Diagram For the Continuous Contact Electrode

Horizontal scale - Time (5 micro seconds/cm)
Vertical scale - Voltage (20 volts/cm)

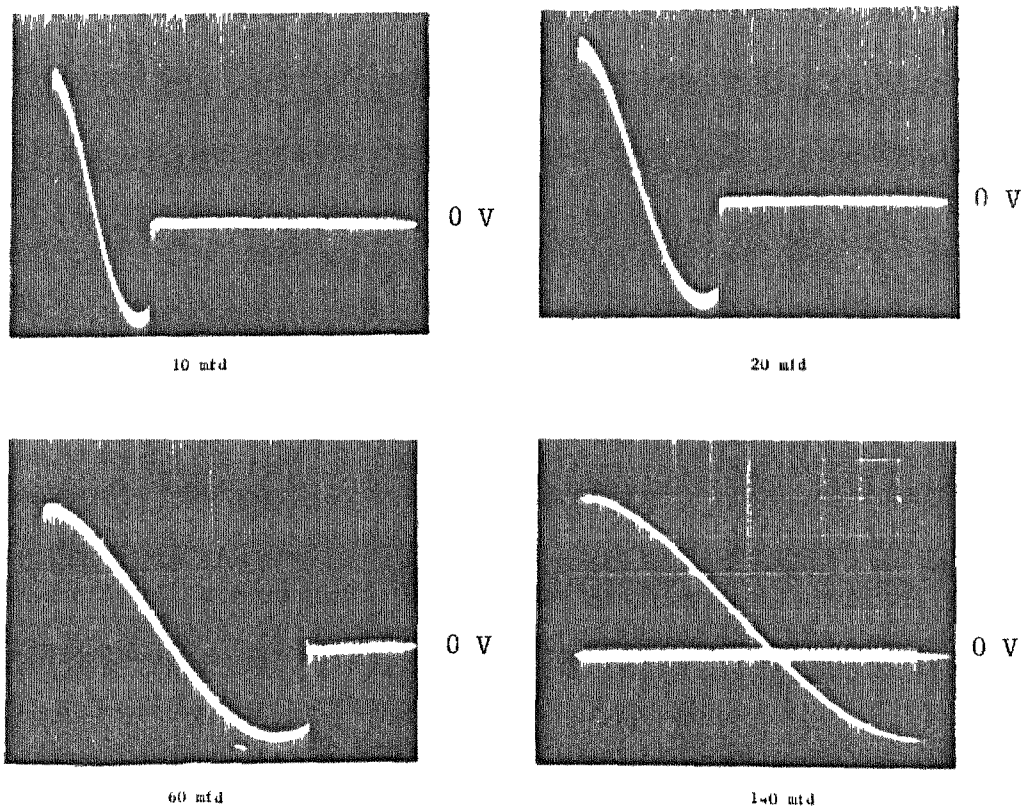

10 mfd 20 mfd

60 mfd 140 mfd

Fig 5.3--Pulse Duration For Varying Values of Discharge Capacitance

6 METHODS OF APPLICATION

When the electrode is in continuous contact with the substrate, a horizontal motion is necessary to prevent welding of the electrode to the substrate. A concentrated effort was made devising different methods of scanning the electrode over the work surface. For each motion type, a different machine was constructed and automated as much as possible to mitigate variability in the coatings.

The electrode scanning motions investigated were either rotary or linear. Each motion type has advantages and disadvantages and each successive machine was built to minimize the disadvantages of the previous one. The reason for using different scanning motions is to vary the duration of the hot spot at either the substrate or electrode surface. The deposition characteristics depend on the degree of local heating, which varies with the particular scanning motion.

6.1 Rotary Motion

The first application device built was a rotary motion machine. A hollow electrode is held in the drilled armature shaft extension of a variable speed DC pancake motor. The motor is attached to a linear bearing slide with an adjustable tilt angle for varying electrode pressure by using a gravity component. The electrode contacts the vertically oriented substrate surface at the tilt offset angle, so there is a line rather than an end area contact at the interface. A 6.35 mm hollow electrode is used, which allows an internal gas flow. Power is supplied to the electrode by a

carbon brush slip ring. Scanning is done by mounting the motor/electrode assembly on a horizontal, reversible table, and the substrate sample on a vertical slide which is stepped by hand at each reversal of the electrode scan. Horizontal feed rate and reversal points are continuously adjustable.

Advantages of the rotating electrode machine are:

1. High deposition rates - a line of contact electrode has a higher power flux than a full area contact electrode.

2. Reproducible cover gas flow - internal flow can be regulated and repeated with greater accuracy than external flow.

3. Larger diameter electrodes can be used - less change time and greater durability result.

4. Continuous, adjustable pressure on the electrode - optimum electrode pressure can be easily maintained.

5. Symmetrical wear of the electrode - a desireable condition for an automated process.

Disadvantages associated with this system are:

1. Carbon brush resistance build-up due to contamination - Any impedance in the discharge path will result in a significant drop in deposition, which is likely to occur when using a brush for power transfer. Drops in deposition

have been noticed when soldered ends instead of bare wire terminations were used in electrode power lead connections.

2. Single electrode scanning - the path width of a single electrode is less than half its diameter while coating, and can inhibit productive capacity.

A refinement that eliminated some disadvantages of the full rotary electrode was to use a reversible rotary electrode as shown in Fig 6.1. This device is identical to the rotating electrode machine except for the motor. A stepper motor is programmed to rotate 360 degrees, reverse, rotate 360 degrees, reverse etc. Since there is never more than one full rotation of the electrode, it can be wired directly to the power source, avoiding the intermediate brush connection. Cooling, if desired, is done by wrapping a coil around the electrode holder. The intermediate electrode motion is controlled to give an oscillating step, two steps forward for every one back. The oscillation keeps the hot spot at the same location on the electrode longer than the full rotary does, without allowing welding to occur. The hot spot of the rotary and rotating-oscillating motion has a scan rate equivalent to the feed rate across the workpiece, as opposed to a rapid scan rate superimposed on the feed rate.

Advantages of the rotating-oscillating electrode machine include (in addition to those of the rotating machine):

1. A direct wired electrode.

2. Better control of electrode motion.

3. Optional cooling of the electrode.

A third rotary motion device was made which has the electrode fixed, but spinning in a circle, similar to a machining tool called a flycutter. The electrode holder is connected to a rotating bar by a flexible junction with enough compliance to follow an uneven work surface. The rotation axis is tilted slightly, which allows two electrodes to be mounted at opposite ends of the bar, alternately stroking across the work surface. Any number of electrodes can be mounted in a circle as long as the power source is adequate. Power is supplied to the electrodes through a brush. The rotation and feed rates are both controllable, and the path swept is nearly equal to the diameter of the circle. Broad areas are covered in a single pass of the electrodes.

Advantages of a flycutting motion machine are:

1. High production rate - a potentially large number of active electrodes and a wide swept path will decrease coating time.

2. Easily adaptable to machine tools - could be directly fitted to a vertical mill.

Disadvantages of this machine are:

1. Brush resistance and contamination.

2. End area contact - power flux is not as great as a line contact.

6.2 Linear Motion

It was of interest to compare a linear motion scan to the rotary, and three different machines were made for this investigation. The first used an adjustable cam to reciprocate a linear bearing slide mounted on parallel rods. The stroke length is set with the cam and the reciprocation rate with a controllable DC motor. A pivoting lever arm attached to the slide holds the electrode and allows a spring constrained vertical motion, giving the electrode compliant, but steady pressure against the substrate, which is mounted on a horizontally moving table beneath the electrode. The table feed and reversing points are continuously adjustable. The electrode/cam assembly is mounted on a slide which is manually adjustable in the vertical direction.

Stroke length is adjusted for the width of the sample and feed reversal points are set for the length. The stroke rate of this machine had to be set at a high rate to overcome stick-slip motion due to low motor torque and tendency of the electrodes to stick to the work surface. The hot spot moves relative to the substrate at an average of 10 cm/sec, a significantly higher rate than the rotary machines which move an average of 0.5 cm/sec.

The stroke velocity is not a constant with this cam. There will be a dead spot at each reversal, during which the electrode does not move. The velocity will build to a maximum during 90 degrees of rotation, and then drop to zero again after a 180 degree rotation. A device was added to the shaft of the drive motor which sensed the reversal points and shut down power to the electrode, so that sticking would not occur at the dead spots. The overall deposition decreased significantly with this switch because the percentage of power down time was high for the short stroke length being used and possibly because the highest deposition occurs at the reversal point, so its use was discontinued.

Power is wired directly to the electrode which scans with an end area rather than a line contact. The greatest coating efficiency is obtained by using 3.175 mm electrodes, although the advantage of internal gas flow through a hollow 6.35 mm electrode is lost by using the smaller electrodes. This apparatus was used for many of the test coatings because it has a fully automated cycle and results were consistent and reproducible.

Advantages of a linear cam stroke machine are:

1. Wide range of parameter control.

2. Direct wired electrode.

Disadvantages are:

1. Uneven stroke velocity - the cam transfers velocity from zero to maximum in 90 degrees of rotation.

2. Dead spots occur during reversal.

3. End area contact of the electrode.

To circumvent the problem of uneven velocity in the cam stroke, another reciprocating device was made which utilized a screw device similar to a "levelwind", which converts rotary to linear motion and reverses itself automatically at motion extremes. Fishing reels use a levelwind to wrap line evenly back and forth along their spindles. The levelwind has a fixed stroke length, but is available in a variety of sizes. There is a dead spot during reversal, but it dwells for a shorter time than the linear cam device does. A fixed speed DC motor is used to drive the levelwind, as shown in Fig 6.2.

A platform connected to the levelwind is reciprocated with dual electrode holders attached to small, low friction air cylinders that apply a regulated pressure to the electrodes. The upper platform acts as the connection point for the cylinders and the lower platform acts as a guide for the electrode holders. The electrodes are free to move vertically within the stroke limit of the air cylinder and have a constant pressure over the full range of travel.

Solid 3.175 mm diameter electrodes were chosen as a standard size most suited to the end area contact motion, being sufficiently large to prevent fracture and erode slowly, but small enough for a sizable power flux and high deposition rate. Gas flow must be external when using solid electrodes. A skirted cup is used to contain the cover gas and purge air from the contact area. Power to the electrodes is wired directly from the source.

Advantages of the levelwind machine are:

1. Even stroke velocity.

2. Accurate, adjustable electrode pressure.

3. Direct wired electrode.

Disadvantages are:

1. Single stroke length and speed.

2. Limited motion - some electrodes stall the stepper motor or cause a stick-slip motion because of extreme sticking.

3. End area contact of the electrode.

A third linear device constructed uses two electrodes mounted on linear bearing slides which are pivoted at one end and driven at the other, as shown in Fig 6.3. The pivot point is a flat spring made of epoxy glass laminate which allows vertical deflection of the slide, but is very stiff in the lateral direction. The driver is a variable cam actuating a pushrod which is connected to the center of an H-shaped yoke assembly. The slides are mounted between the upper and lower legs of the H in bearings and the legs of the H are independent links with a bearing connection at the center bar. From a side view, the H can buckle in two directions, forward or rearward or stand straight up. Choosing the zero spring deflection point at the two extreme pushrod locations and corresponding buckled positions of the H means that the maximum spring deflection occurs at the midpoint of pushrod travel or when the H side profile is straight. Using this geometry partially cancels out the dead spots of the crank and linkage mechanisms.

The stroke length of the electrodes is determined by the amount of deflection at the driven end of the slide, which is governed by the stroke length of the cam/rod driver. The maximum electrode stroke length was set at 6.35 mm to prevent interference between the two slide assemblies.

One cam revolution corresponds to two deflection cycles of the electrode, so the stroke frequency is double the cam revolutions. A single speed stepper motor drives the cam at 300 RPM so there are 600 full strokes (up and down), or 1200 single strokes per minute per electrode. With a 6.35 mm stroke, the electrode velocity is 12 cm/sec relative to the work surface.

The electrode holders are mounted on the free moving part of the linear bearing slide and are connected to air cylinders which closely regulate the electrode contact pressure against the work surface. Since the stroke motion moves about a pivot point, the electrodes are in a line contact rather than a full end area contact with the substrate, maximizing the power flux. Electrodes 3.175 mm in diameter are wired directly to the power source, and are mounted above one another with a 25 mm spacing to provide clearance for the slides and holders.

The electrode/slide/cam assembly is then mounted on a linear motion device called a Uhing Variable Pitch Traverse, manufactured by Amacoil (34). This device converts rotary to linear motion with contained roller bearings canted at an angle and in contact with the rotating shaft. The bearings track along the shaft at a speed dependent on the angle of contact. A preset stop reverses the contact angle and direction of travel while the shaft rotates with a constant speed and direction.

Advantages of this linear-oscillating machine are:

1. Controllable parameters - stroke length and speed, feed rate and electrode pressure are all adjustable.

2. Line contact electrodes.

3. Direct wired electrodes.

Disadvantages are:

1. Wide spaced electrodes - some overlap is necessary for a complete coating.

2. Electrodes jam on sharp edges - the positive pressure on the electrodes causes them to hang up on projections rather than move over them.

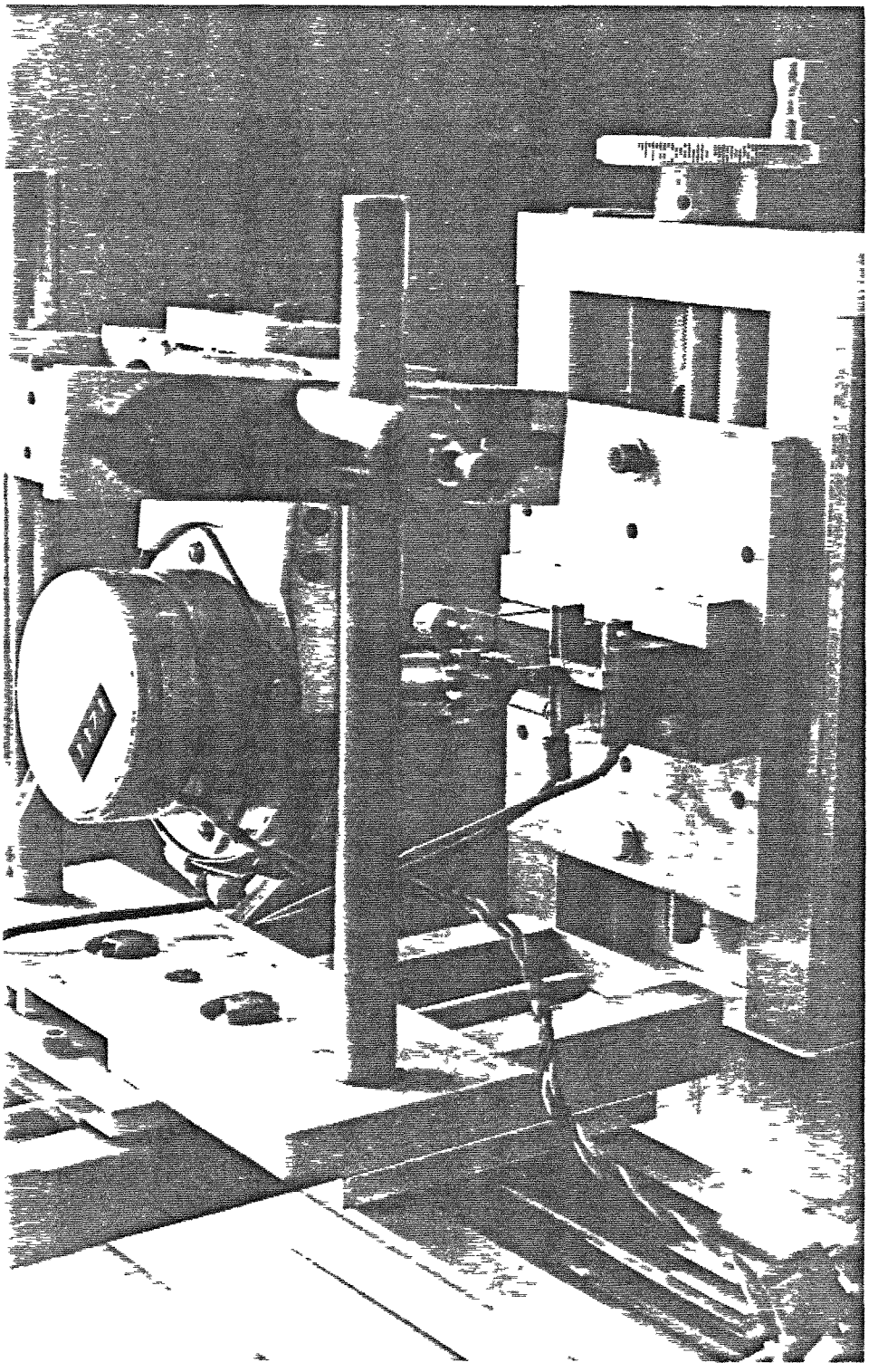

Fig 6.1--Rotating-Oscillating Applicator

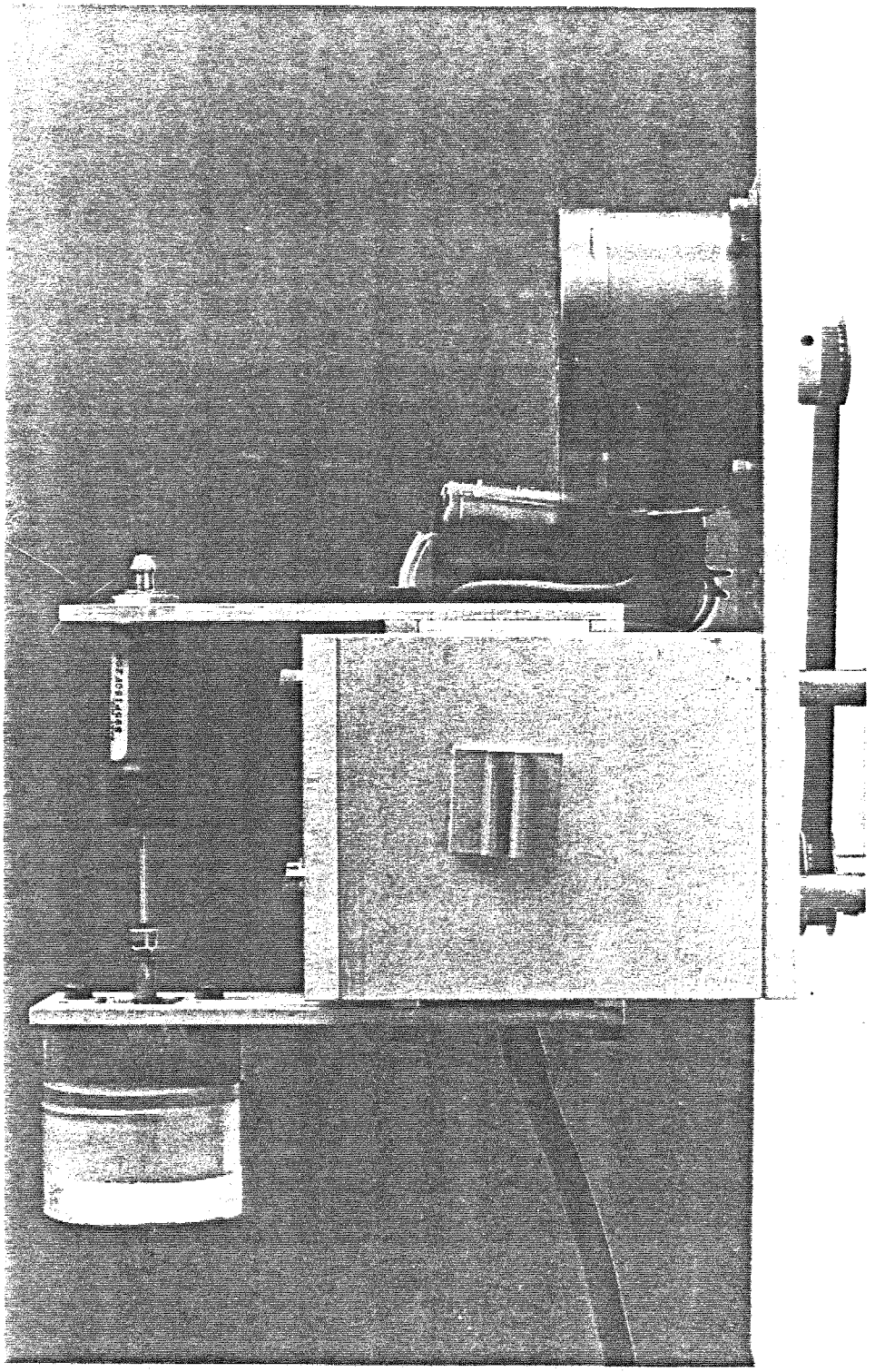

Fig. 6.2--Levelwind Applicator

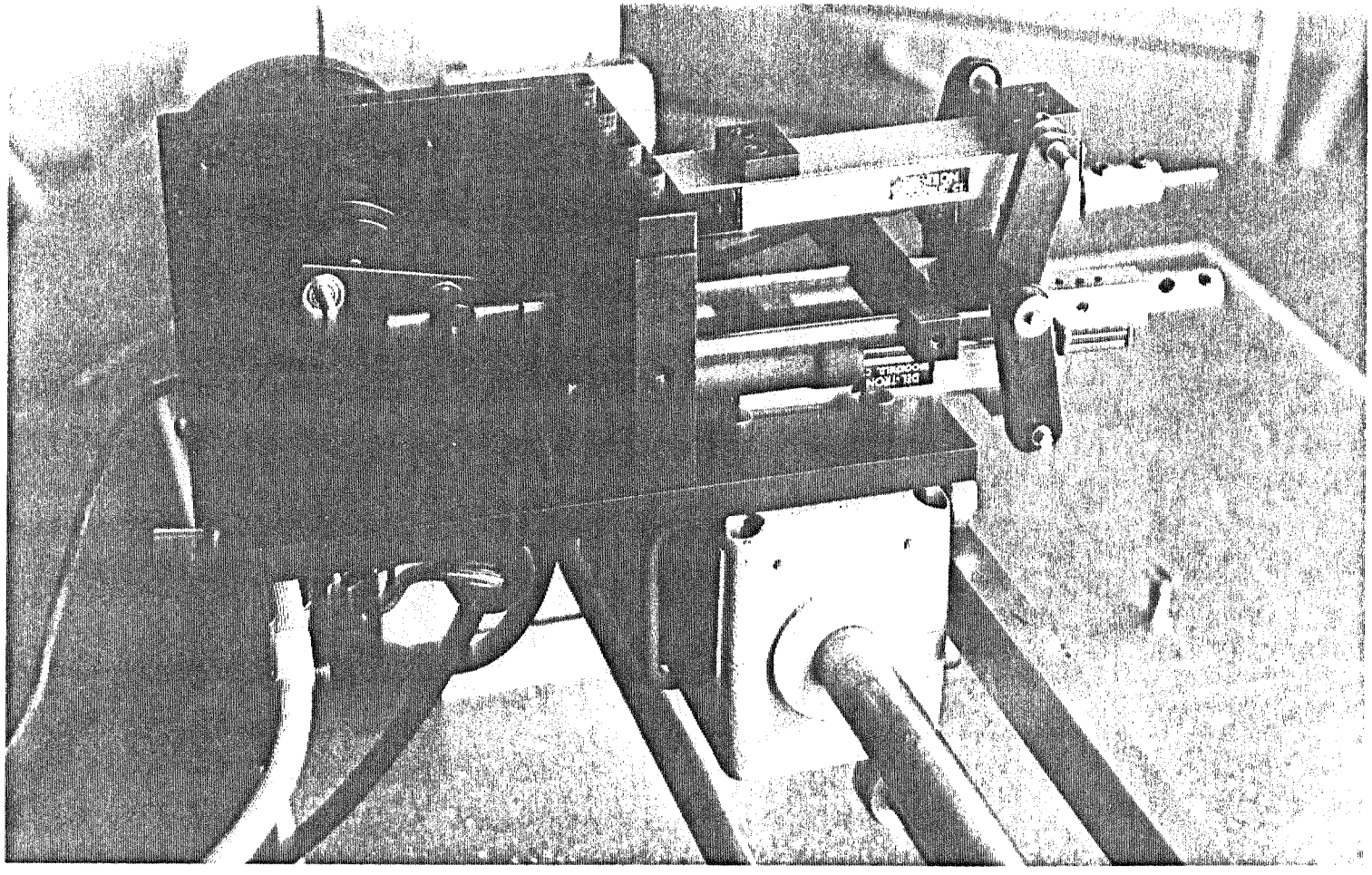

Fig 6.3--Linear-Oscillating Applicator

7 DEPOSITION MECHANISM

Explanations of the transport mechanisms in the ESD process are few and do not elaborate beyond a general overview (4)(7). From observations during this research, conclusions have been drawn which place the ESD mechanisms in a general class of phenomenon associated with plasma-arc discharge as found in processes such as electric welding and electro-discharge machining (EDM). By demonstrating a similarity between these processes, the larger amount of research done on plasma-arc discharge can be used directly to explain the ESD mechanisms. A detailed analysis will not be presented, but rather sufficient parallels will be drawn to show that ESD is most likely a micro-welding process.

The deposition mechanisms are all related to the temperature at the electrode-substrate interface. The sources of heat are current flowing across and chemical reactions occuring in the interface area. Current can flow through a direct contact of asperities or across a gap of ionized gas. The balance of these modes of heat determines the deposition characteristics. The balance is affected by a multitude of conditions (20)(24)(29):

1. Electrodes and substrate : thermal conductivity, melting point, electrical resistivity and contact area.

2. Atmosphere : conductivity, ionization and dissociation energies and reactivity with electrode and substrate.

3. Output power : energy, duration and frequency.

4. Electrode motion and pressure : movement of the hot spot relative to the electrode and substrate and the normal force between electrode and substrate.

A change in any one of the four major conditions will result in a different quality and/or quantity of deposition, and a number of different changes are possible for each condition.

7.1 Electrodes and Substrate

Characteristics used for comparing different electrodes include volume deposited, presence of lumping and degree of sticking at various power levels. The volume deposited is used as a measure of transfer efficiency. This, in addition to wear testing, is the most useful measure of performance when varying the four main conditions. The elemental electrodes tend to deposit less than the carbide and nickel/cobalt base electrodes, and in many instances a net weight loss of the substrate occurs. The elemental electrodes (molybdenum, tantalum and niobium) have high melting temperatures and are similar to non-consummable electrodes in conventional welding processes. The 316 stainless substrate boiling point is near the melting point of the elemental electrodes, and often the electrodes have a net weight gain, presumably from the substrate.

Nickel and cobalt binders used in carbide electrodes have half the melting temperature of the elemental electrodes, so the carbides tend to deposit more heavily than the elementals. The heaviest deposits are gained with nickel/cobalt base (T-700 and Stellite) electrodes. Differences in electrical and thermal properties account for variations in deposit of electrodes with the same melting point (27).

The current density is an important factor in determining the temperature at the interface, so an electrode with a line contact will generate much higher temperatures at the same power level than an end area contact and results in a larger deposit. Too high a temperature will cause lumping, however.

Lumping, as shown in Fig 7.1, is a series of isolated bumps that form when a limiting value of power is exceeded. This limiting value is different depending on the major conditions in force at the time. The nickel/cobalt electrodes tend to lump heavily, the carbides moderately and the elementals not at all. Welsh has encountered lumping in his research and notes that of the carbides, titanium carbide has the greatest tendency to lump (6)(7).

The resistance of the electrode to scanning motion (stickiness) depends on the composition of the substrate and the electrode. Generally the high deposition, low melting point electrodes have more resistance than the higher melting temperature electrodes when scanning 316 stainless steel. Sticking is most likely due to molten areas freezing rapidly enough to arrest motion before the next pulse, and the larger the molten area, the

greater the resistance. A scanning motion of the electrode is required to break these micro-welds or a continuous short circuit will occur and the electrode will not move or melt.

7.2 Atmosphere

Variations in atmosphere should cause a change in deposition characteristics similar to a plasma-arc if a spark discharge is occuring at the electrode-substrate interface (24). This is indeed the case. The differences when using an argon cover as compared to air are:

a. Deposition decreases by 20-30 percent.
b. Lumping is reduced or eliminated.
c. The appearance of the coating is more even, smooth and clean.
d. Stickiness is decreased.
e. The spark changes color from yellow to blue and is more intense.

Using oxygen as a cover gas has one major effect: lumps form immediately, except when using the elemental electrodes.

The effect of argon can be explained in terms of changes in the plasma-arc. Argon ionizes more readily than diatomic gases because dissociation need not occur before ionization. A stable conducting path is formed which allows arcing to occur at a lower voltage (25). The electrode transfer characteristic when using argon is that of a fine spray of droplets, whereas in the presence of dissociable gases, a globular transfer is predominate. The spray transfer is primarily due to the low thermal

conductivity of the argon plasma (25)(26)(27).

The fine matte appearance of the ESD coating is likely due to a spray transfer, whereas the splashed droplet formations are the result of globular transfer. Comparison of a deposit with argon to one without shows larger areas of spray deposit using argon, even extending outside the droplet formations. Fig 7.2 illustrates three single pass electrode paths using a CA-815 electrode and the rotating-oscillating applicator. The top path is the electrode contact area with no power being applied. The middle path uses a power setting of 138 watts and no cover gas, while the bottom path uses the same power with argon as a cover gas. The difference in pathwidth for the middle and bottom paths is shown in Fig 7.3 and Fig 7.4. At higher magnification, Fig 7.5 shows the non-argon path to be strictly delineated between the deposit and substrate, whereas the argon cover shows a less defined boundary with a spray formation superimposed over heavily impacted droplets and the substrate in Fig 7.6.

The splashed appearance of the globular formations arises from a plasma jet which forms behind the droplet after separation from the electrode, accelerating the droplet into the substrate (30). As the plasma jet increases in velocity, a transition from globular to spray transfer occurs (27), which would explain why many times the droplet formations have a superimposed matte finish.

It is likely that the majority of electrode mass is transported by globular transfer, with spray transfer contributing a only a minor amount. This would explain the decreased deposition encountered when using an argon

cover gas. Globular transfer is associated with high thermal conductivity plasma formed by dissociable gases and a high energy dissipation in the arc column (27). Lumping seems to be an extreme form of globular transfer occuring in the presence of oxygen. The oxygen can add a high energy to the arc column from the heat of formation of oxides, similar to the principle of an oxy-acetylene cutting torch (24). Dissociated oxygen and metal ions in the arc react readily to form oxides in a strong exothermic reaction. Of the metals possibly present, iron and titanium have the largest number of oxidation states possible in the arc temperature regime. Titanium has the highest heat of formation, 587,980 gram-calories per mole of oxygen (23), which tends to confirm Welsh's observation of the high lumping tendency of titanium carbide. Injecting argon into the arc column displaces oxygen, resulting in fewer reactions, thereby decreasing the cathode temperature and nullifying the lumping.

The spray transfer associated with argon should give a smoother coating than a globular transfer. The clean appearance of the coating is possibly due to a cathodic etching effect (31). The stickiness should decrease as well as there is less globule area to freeze. Since the conducting path of the arc changes properties with the inclusion of argon, the spark color and intensity should change as well.

7.3 Output Power

The output power is the most easily controlled condition of the four. Ideally, the maximum power level should be at the onset of lumping or when the transfer efficiency begins to decrease. Lumping can be mitigated

without the use of argon if the pulse duration is decreased sufficiently, perhaps because a short duration pulse does not allow sufficient time for oxide formation and the attendant increase in temperature needed for lumping to occur. With a short duration pulse, the transfer efficiency starts to drop before the onset of lumping, so an argon cover gas is not necessary. The pulse energy can be maintained by increasing the voltage level as pulse duration decreases, thereby not sacrificing any power capabilities.

7.4 Electrode Motion and Pressure

Motion of the electrode relative to the substrate probably functions to initiate spark discharge, similar to striking an arc in electric welding. Relative motion between electrode and substrate also acts to distribute heat between the two. The hot spot moves rapidly in relation to the electrode and slowly in relation to the substrate with a fully rotating electrode that slowly scans the substrate. Just the reverse occurs with a fixed electrode that rapidly scans the substrate. Several relative motions are possible between these two extremes. The relative distribution of temperature will influence the transfer mechanisms at the interface and plays an important role in the ultimate deposition.

The pulse discharge melts or vaporizes contacting asperities and increases the gap distance between the electrode and substrate. Pressure on the electrode is important in maintaining a consistent gap across the interface during discharge. The main concern is having too light a pressure, which will cause bouncing and non-contact of the electrode, leaving an uneven coating. Too heavy a pressure creates undue friction and

stress on the electrode and does not allow a good spark. The range of useable pressures for consistent results is relatively broad, and when easily controlled, a normal load of 100 grams or 10.8 kPa (1.5 psi) pressure acting on a 1.27 cm (0.5 in) diameter piston was used.

7.5 Transfer Efficiency and Deposition Rate

The transfer efficiency is the ratio of weight gained by the substrate to the weight lost by the electrode. As a general rule, efficiency decreases with the addition of argon as a cover gas and after the voltage setting exceeds a limiting value of about 220 volts, assuming that lumping does not occur. Fig 7.7 lists the efficiencies of various electrodes with and without an argon cover gas, using the rotation-oscillation applicator. Efficiencies were measured at 180 volts across a 10 micro-farad discharge capacitor with a pulse rate of 850 Hertz. For the majority of application devices, molybdenum exhibits a negative efficiency both with and without an argon cover gas, associated with a net weight loss from the substrate. The highest efficiency was obtained with CA-815, ranging from 20-40 percent greater than the other electrodes.

The transfer rate indicates the suitability of the electrodes for productive application. The rate can be compared either as a volume per unit time or a volume per unit pulse energy.

The time rate is computed by:

$$\text{cu cm /sec} = (\text{mg/min})*(1/\text{density in grams per cc})*(1/60000) \quad (7.1)$$

The energy rate is computed by:

$$\text{cu cm /joule} = (\text{cu cm /sec})*(1/\text{watts}) \quad (7.2)$$

where,

watts = energy per pulse times discharge rate (joules)*(pulses/sec)

The energy rate can be interpreted as both an energy efficiency of the electrode and as a rate of deposit of the electrode at a unit power setting.

Fig 7.8 illustrates the relation between the time rate of deposit versus the energy per pulse for a CA-815 electrode with an argon cover gas, again using the rotation-oscillation device. A 10 micro-farad discharge capacitor is indicated by squares and a 20 micro-farad discharge capacitor by triangles in the plot. Note the strong linearity between the deposition rate and energy for the range of energies most often used in this research.

The deposition rate for several electrodes is shown in Figs 7.9, 7.10 and 7.11 using the linear cam, levelwind and rotation-oscillation applicators respectively. Side-by-side comparisons are made for deposition with no cover gas and for the effect of adding an argon (or oxygen) cover gas. The rotation-oscillation device was the only one of the three applicators which used the short duration pulse output.

Raw data consists of a weight in milligrams deposited at a particular voltage, capacitance and frequency for a given time in minutes. Each datum is converted to a deposition rate by using equations 5.1, 7.1 and 7.2. The deposition rate values are segregated by electrode, application device and cover gas, and then averaged. This average deposition rate is what appears in the plots. The analysis of data for these graphs assumes linearity of deposition rate and energy over the range of power used in the tests.

Electrodes common to all three plots are CA-815, R-241 and Molybdenum. Comparison shows the CA-815 and Molybdenum to have wide ranging deposition rates for each of the applicators, whereas R-241 is fairly consistent with all three. The largest rate is obtained with T-700 and the linear cam device, which has the highest electrode surface velocity of the three applicators.

CA-815 deposited with an argon cover gas has the highest deposition rate with the levelwind and the lowest with the linear cam, probably due to the higher argon flow rate through the hollow electrode used with the linear cam. The incidence of lumping is high with this electrode unless a shortened duration pulse or an argon cover gas is used.

The R-241 electrode is consistently low in deposition rate between the three applicators, although the percentage changes are significant for deposits with an argon cover applied with the levelwind. The electrodes T-700 and Stellite have a high lumping tendency and should be retested on the linear cam and levelwind using a short duration pulse. A significant increase in deposition without lumping should be the result.

The rapidly moving hot spot of the linear cam appears to deposit T-700 and the elemental electrodes better than the other applicators. The levelwind favors the carbide electrodes whereas the rotation-oscillation applicator deposits best with the CA-815 electrode.

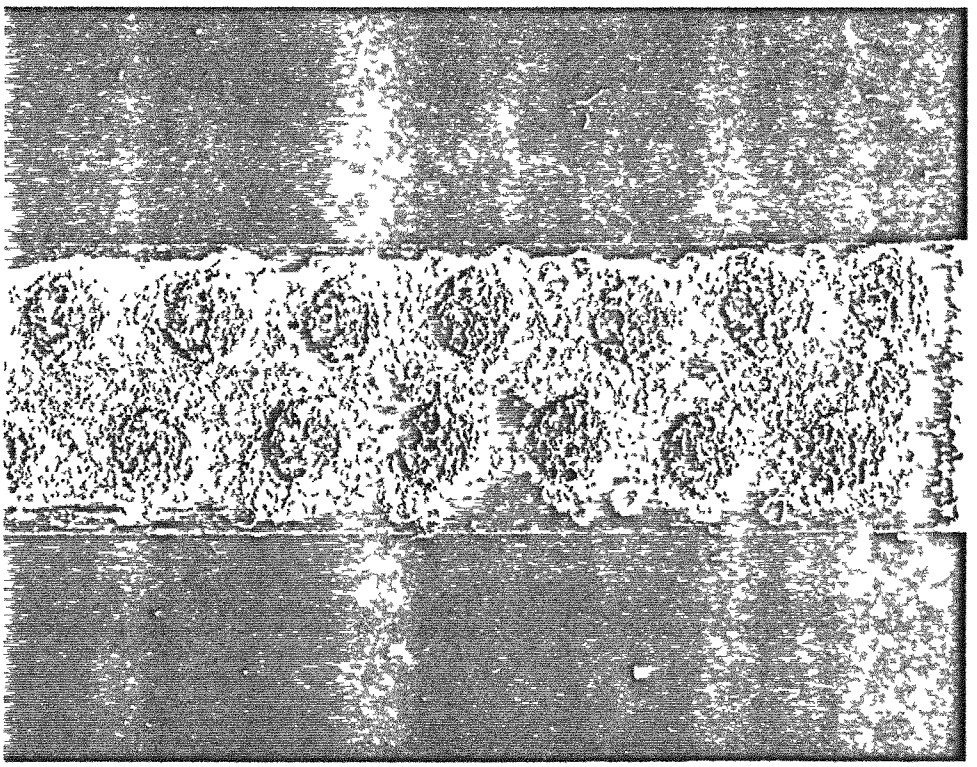

Fig 7.1--Lumping On the Substrate

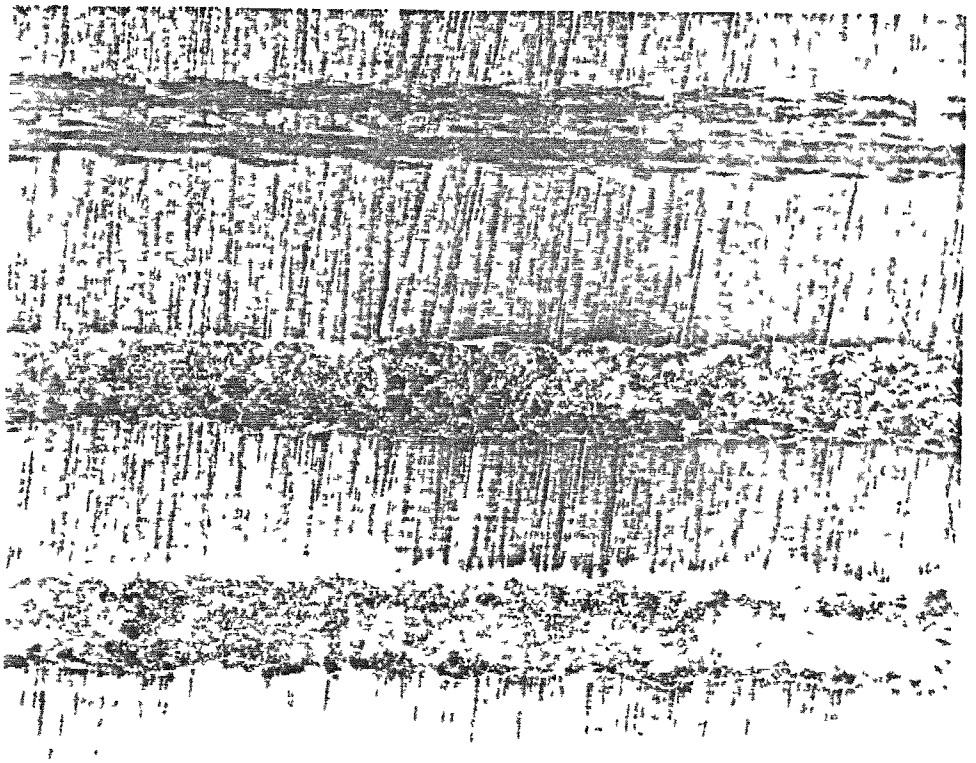

Fig 7.2--Deposition Tracks

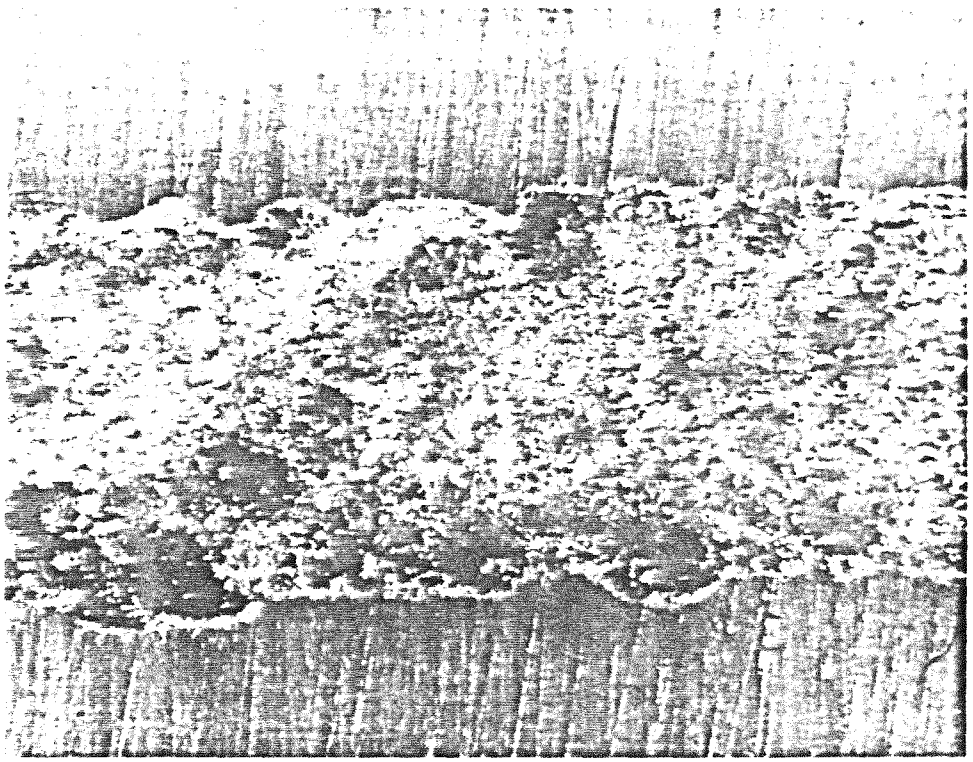

Fig 7.3--Deposition Track With No Cover Gas

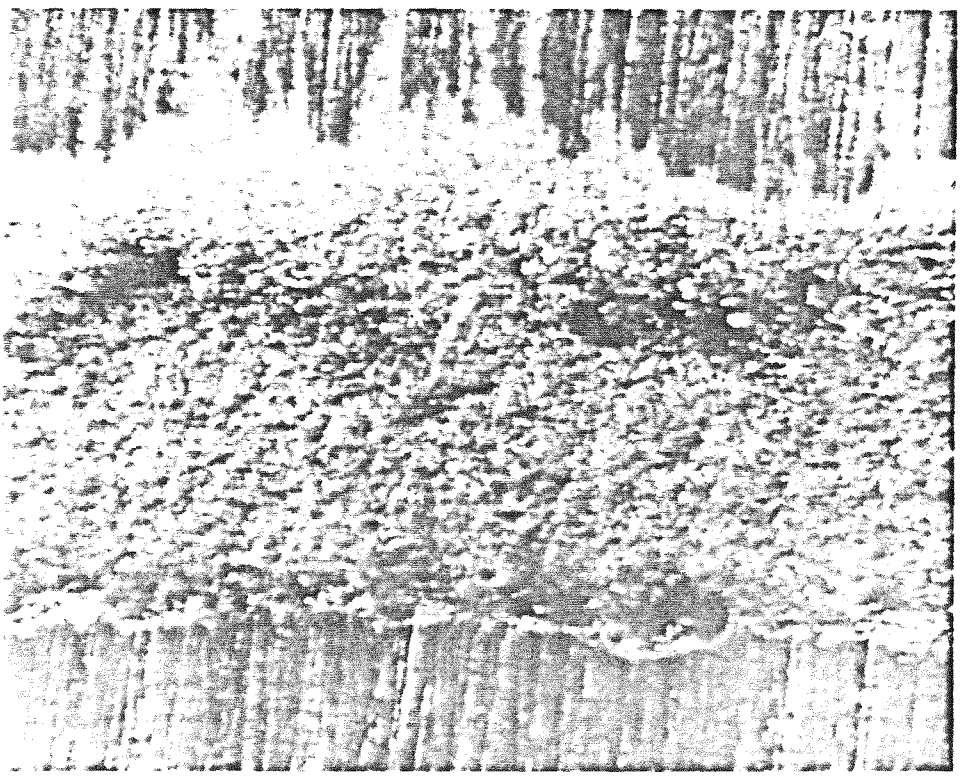

Fig 7.4--Deposition Track With an Argon Cover Gas

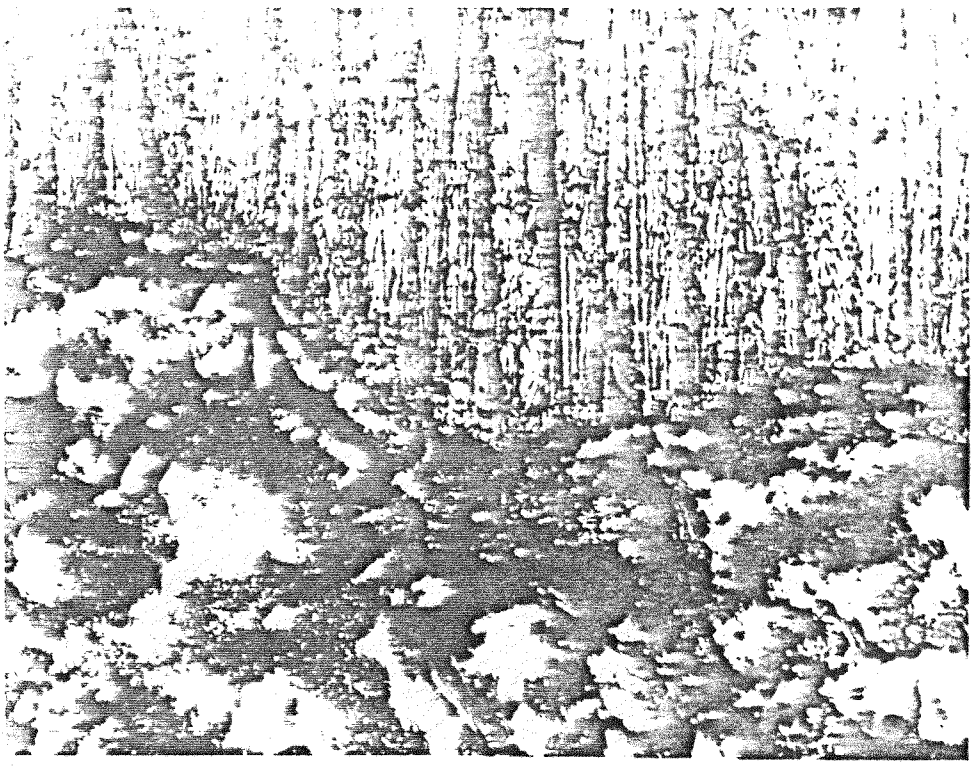

Fig 7.5--Edge of Deposition Track With No Cover Gas

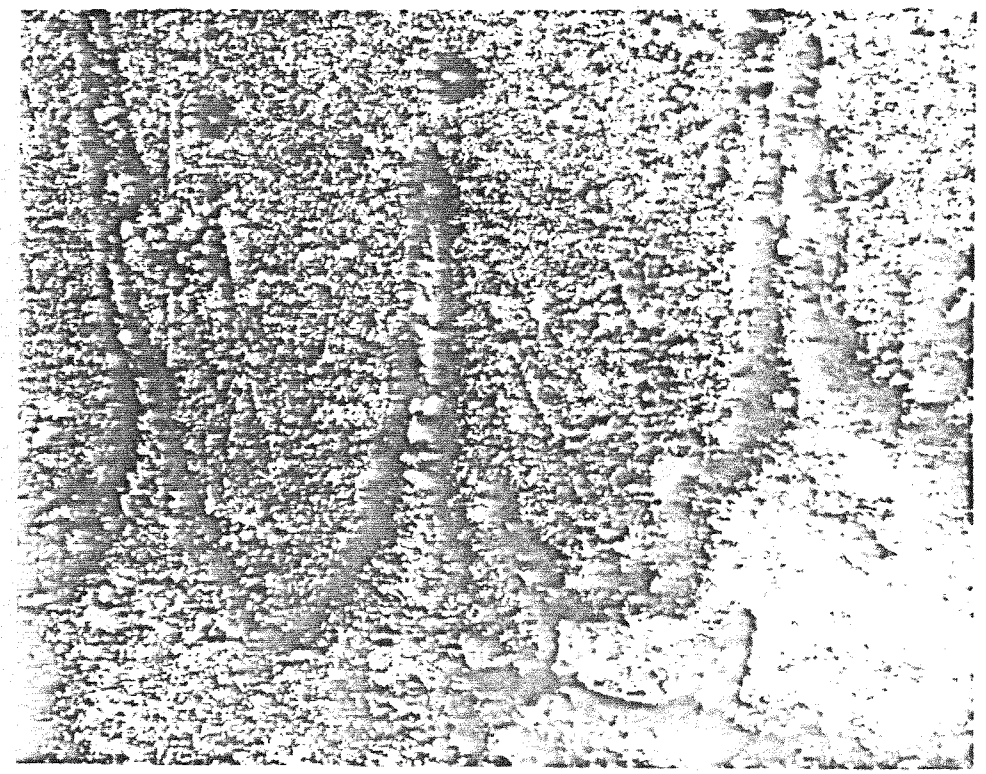

Fig 7.6--Edge of Deposition Track With an Argon Cover Gas

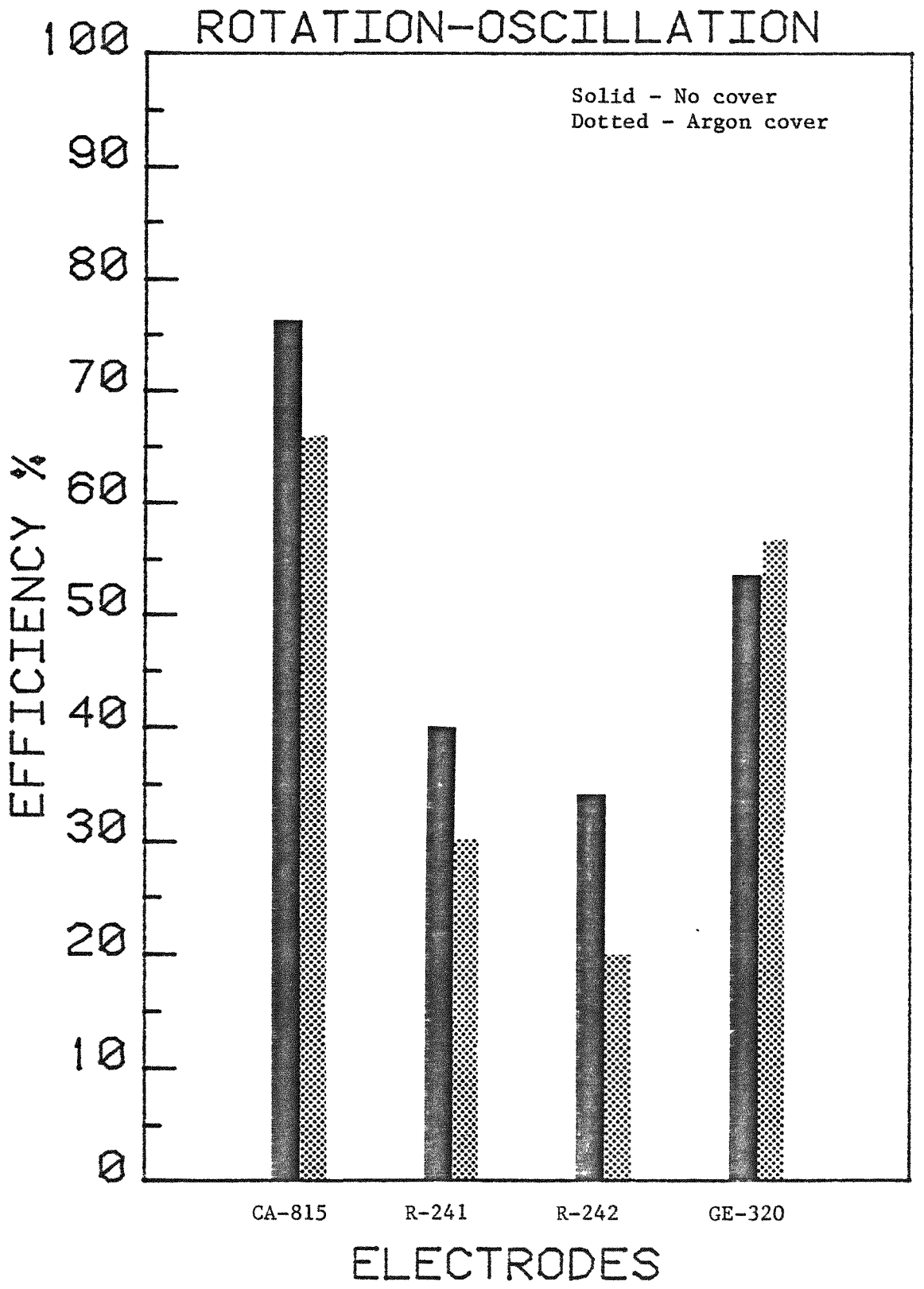

Fig 7.7--Mass Transfer Efficiency of Electrodes Deposited With the Rotation-Oscillation Applicator

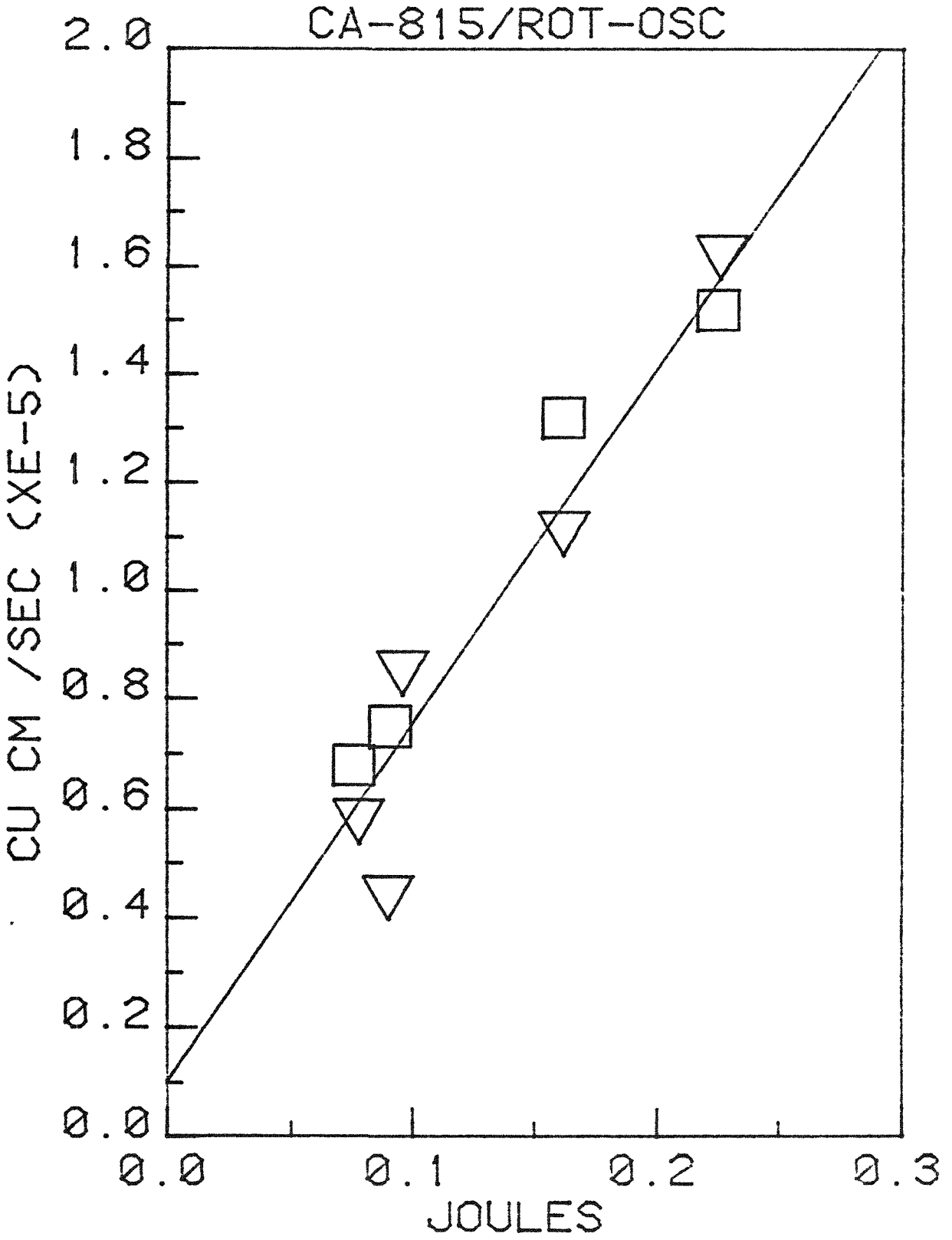

Fig 7.8--CA-815 Electrode Deposition Rate versus Energy
Using the Rotation-Oscillation Applicator

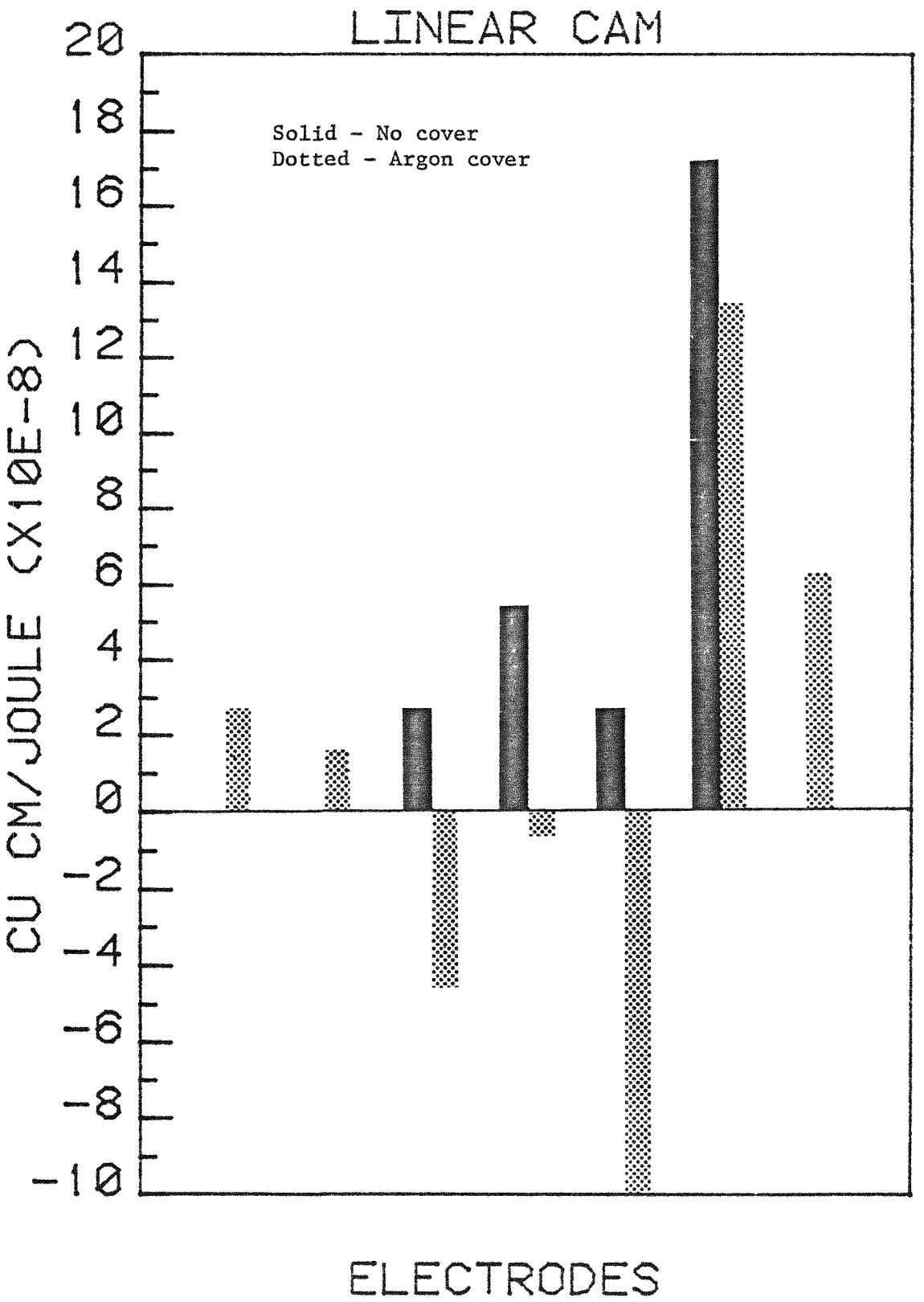

Fig 7.9--Electrode Deposition Rate versus Energy Using the Linear Cam Applicator

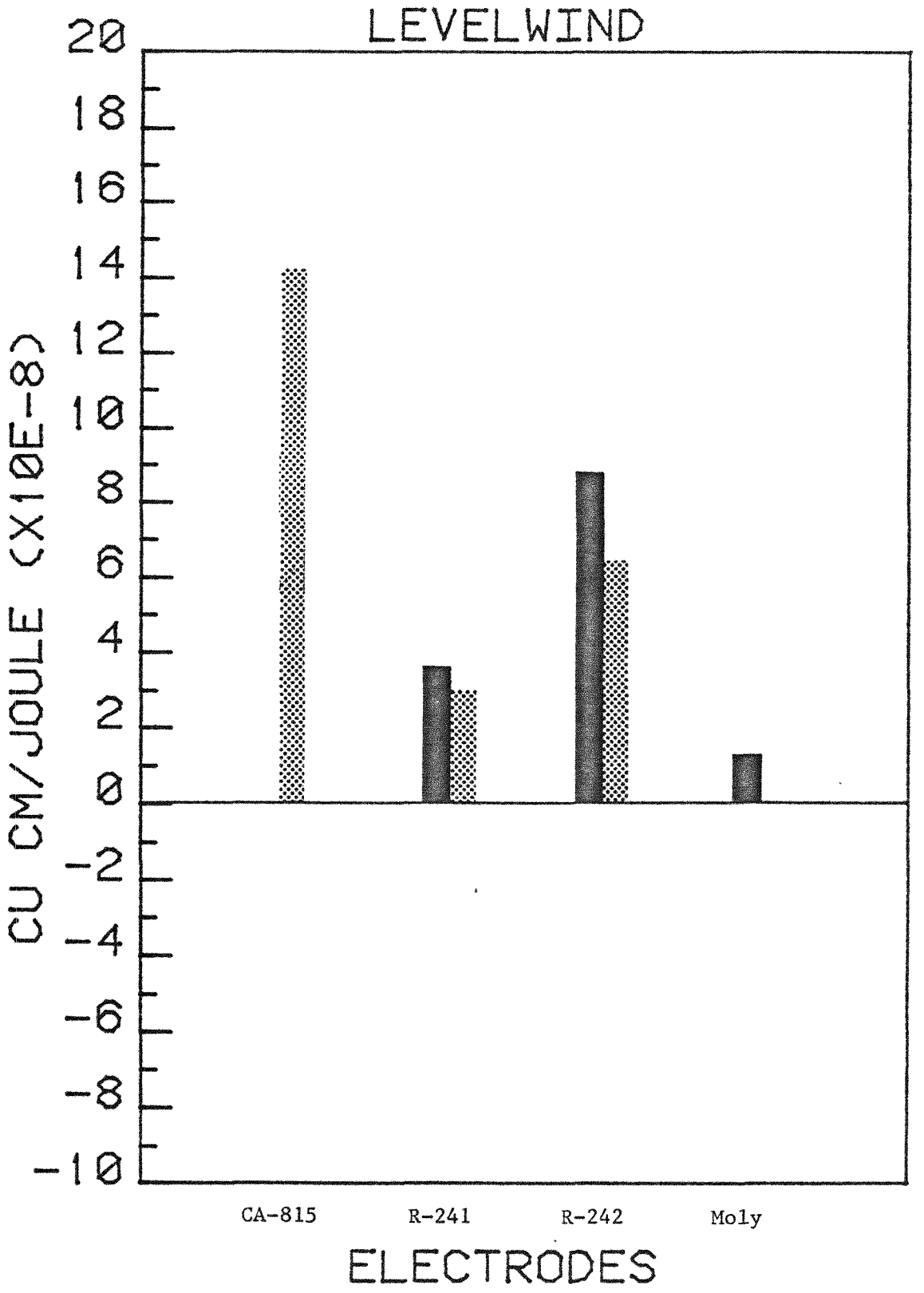

Fig 7.10--Electrode Deposition Rate versus Energy Using the Levelwind Applicator

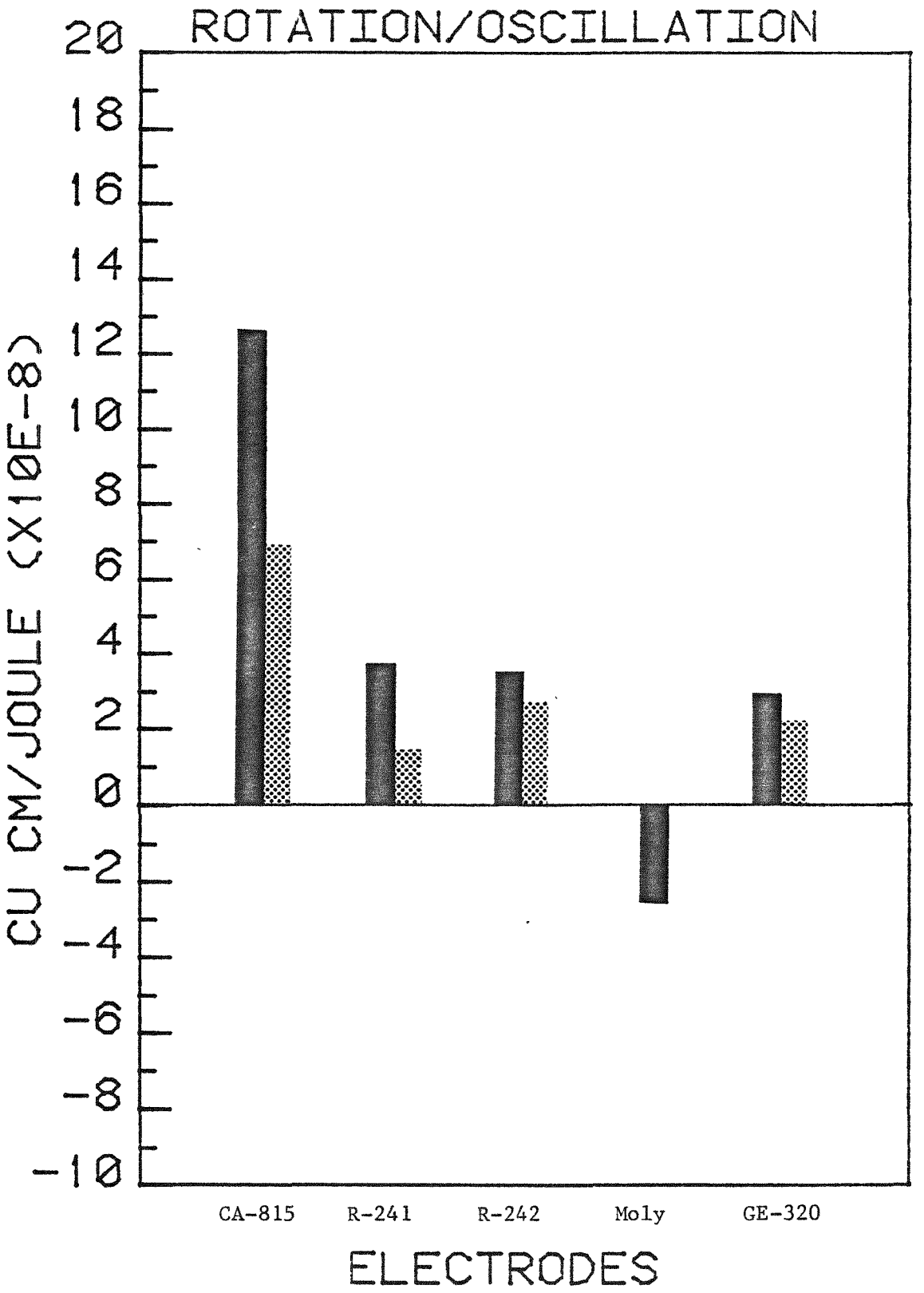

Fig 7.11--Electrode Deposition Rate versus Energy Using the Rotation-Oscillation Applicator

8 FRICTION TESTING AND WEAR RESULTS

Evaluation of a thin coating characterizes such properties as hardness, wear resistance, friction coefficient, bond strength and surface topography. If hardness is measured by indentation, the coating should be at least four times the indentation depth of penetration (17). Measuring the hardness of an ESD coating is done by sectioning the sample and doing a Knoop hardness test across the substrate/coating boundary, as shown in Fig 8.1. The value of Knoop hardness for an indent load of 100 grams taken along the sectioned coating of different electrodes is given in Fig 8.4. The values range from a high of 1155 kg/square mm for CA-815 to a low of 784 kg/square mm for Molybdenum. The magnitude of surface roughness precludes indenting the coating directly, as the allowable indent depth is on the same order as the roughness. This method is impractical and time consuming for testing large areas. Alternatives include estimating final hardness to be the same as the initial electrode hardness or to simply not determine the hardness directly, but to do comparative testing rather than tabulate absolute values of wear.

Using Archard's wear formula (equation 3.1) requires not only the hardness, but the wear volume, the distance in sliding, the normal force exerted on the coating and the wear coefficient "K". The test apparatus must slide a metal contact over the coating at a known normal load. Because of the high hardness of the ESD coatings, a long distance in sliding is required with light pressures to effect any measurable wear.

8.1 Rotary Cylinder Test

The apparatus used for this test is shown in Fig 8.2. It uses a 1650 RPM motor with a replaceable hardened, hollow 9.525 mm cylinder of heat treated 4130 steel (Rc 50) attached to the shaft. Beneath the shaft and at right angles to it is a swivelling saddle with a milled pocket to hold the coated sample. The saddle is attached to a reciprocating platform which scans the sample back and forth under the rotating cylinder. The motor is mounted on a counter-balanced arm, which after nulling out, has weights attached to give the normal force. The Hertz contact stress associated with a 500 gram normal load is 75 MPa (10.88 ksi) and with a 2000 gram normal load is 150 MPa (21.76 ksi). After the sample is carefully weighed, the cylinder scans the coating for a fixed time. The sample is reweighed and the weight loss and wear volume are determined. Another sample with a similar coating is weighed and tested at a higher normal force until enough data is accumulated to plot a wear vs load curve for the particular coating. Curves are generated for several electrodes and coating conditions and compared in Figs 8.5-8.10.

The wear in these plots is measured as the volume lost per meter of sliding, where the distance of sliding is simply the motor rpm times the circumference of the test cylinder in meters times the test time in minutes. A dashed reference line corresponding to the wear load curve of uncoated 316 stainless steel (Fig 8.5) is included in each graph for comparison. The wear slope of the curve for the uncoated 316 stainless steel is 8.02E-7 cu cm/m-kg. The triangles are actual data points with a linear least square fit line drawn through them. The least wear is exhibited by the R-241

coating with a slope of 0.367E-7 cu cm/m-kg. The elemental electrodes show wear slopes of 2.64E-7 cu cm/m-kg for niobium, 1.464E-7 cu cm/m-kg for tantalum and 1.95E-7 cu cm/m-kg for molybdenum. Finally, T-700 has a 1.75E-7 cu cm/m-kg wear slope.

Some problems which have a significant effect on the data occur with this test. One is build-up of debris on the sample. Adhesive wear occurring with dry metal rubbing will cause asperities to break loose from the substrate and act as an abrasive between the two contacting surfaces. The longer the test is run, the greater the influence of abrasive wear.

Another problem is sample to sample variation of the coating. The entire width of the coating is rubbed off during the test, so a new sample must be used for each increment of normal load. In some cases the problem encountered is that of oxidation as the test proceeds. The high local pressure, surface velocity (82 cm/sec) and resulting temperature of the contact area allows oxidation of nickel and/or iron from the coating or cylinder to build up until it is visible as a brown or black strip. Depending on the load, oxidation can occur 3 to 8 minutes into the test. The oxide acts as a lubricant and greatly decreases the wear of the coatings. Stellite has no readily oxideable elements and wears away in a shorter time than the oxideable coatings. If a nitrogen atmosphere is used to conduct the wear tests, no oxide layer occurs in the other coatings and they wear as rapidly as the Stellite.

8.2 Linear Reciprocating Ball Test

A way to avoid oxidation is to use a high contact stress in order to shorten the failure time. A common wear test is a pin on disc coating evaluation. A spherical rather than a cylindrical wear probe (pin) is used to slide across the sample (disc), which exerts very high Hertzian contact stresses on the coating. The probe moves at a slow surface velocity (4 cm/sec) and does not develop the necessary heat for oxides to form. Based on a pin and disc test similar to one used in a NASA technical report (18), a linear reciprocating ball tester was made, as shown in Fig 8.3. It uses a counter-balanced lever with an adjustable weight at one end and a tungsten carbide ball at the other. Weights are attached midway between the pivot and ball, so the normal force at the ball is one-half the total weight hung. The arm is reduced in vertical section to a thin web between the pivot and weight attachment point, to which strain guages are mounted. A motor and cam reciprocate a linear ball slide on which is mounted a sample holder. The slide moves at right angles to the arm so that the ball tracks up and down the length of the sample. A counter is connected to the slide to record the number of cycles completed.

The wear track of the ball is narrow enough that several tests may be run on the same sample, eliminating variability when making friction coefficient evaluations. The overall test time is short and reliable, making it possible to characterize many coatings without a large investment of time. As in any friction wear test, the most critical part is insuring the cleanliness of the sample coatings. A double soak and final ultrasonic bath in acetone was used as standard procedure for cleaning test samples.

The strain guages measure the horizontal friction force between the ball and coating, which is amplified and recorded on a strip chart. After the arm is calibrated with a known force, a friction coefficient can be computed for the coating from the given normal force and the recorded horizontal force, where:

Friction coefficient f = horizontal force/normal force

This is the same friction coefficient that is used to determine the wear coefficient "K" directly (equation 3.2). The traces of strain guage output give a real time output of friction and wear history of a particular coating, and are reproduced for several coatings with and without a cover gas in Figs 8.11-8.15. These traces are divided into 10, 100, and 1000 cycle sample points and are measured using a normal load of 500 grams on a 5.56 mm (7/32 in) tungsten carbide ball, which exerts a Hertzian contact stress of 1.42 GPa (206.24 ksi). The trace is calibrated for 100 grams force per major division on a plus or minus 500 gram full scale graph.

Coefficients of friction are determined for the trace at each cycle interval by reading an average peak to peak force and dividing by two to get the horizontal component force. The coefficients of friction are detailed in Figs 8.16-8.18 for a variety of electrodes at each cycle interval. The second trace for CA-815 (Fig 8.11) shows the result of light sanding on the coating, which improves the coefficient of friction dramatically at all three cycle intervals. All electrodes at the 1000 cycle interval show a uniform coefficient of friction, likely indicating a wearing in of the coating. Molybdenum with an oxygen cover gas exhibits the lowest

coefficient of any of the coatings at the 10 cycle interval, but increases rapidly with succeeding intervals. The carbides show no consistency in relation to one another as the intervals increase until the 1000 cycle point.

As the horizontal friction force increases, so does the shear stress on the deposited layer. The high Hertzian contact stresses act to separate the coating from the substrate if the interface bond strength is low. The bond strength of the coating can then be evaluated by observing the wear track with an optical or electron microscope. Any layer separation or spalling is visually detectable and can be correlated to a known stress, giving a value for coating adherence to the substrate.

8.3 SEM Analysis

A scanning electron microscope (SEM) is used to record the micro-formations of the coatings and the wear tracks left by the ball test for any signs of spalling. The results are given in Figs 8.19-8.26. The difference in microstructure of an R-242 coating with and without an argon cover gas is shown in Fig 8.19 and Fig 8.20. Note the increased graininess of the droplet structures which were deposited with an argon cover gas. The remaining Figures are records of the wear tracks of some of the traces listed in Figs 8.11-8.15. The relative size scale is located in the lower left corner of each picture. The wear tracks show scattered debris, but have no indications of large scale spalling. In no instance does it appear that the ball has broken through the coating to the substrate. The wear track on the CA-815 coating is not readily discernable in Fig 8.25, although

it is certain that the track passes through the region. The track of the sanded CA-815 coating in Fig 8.26 is similarly difficult to perceive, although its presence is indicated by the debris running in a straight line across the bottom of the photograph. Higher magnifications and many scans of these areas revealed no flattened areas or indications of wear in the track zone.

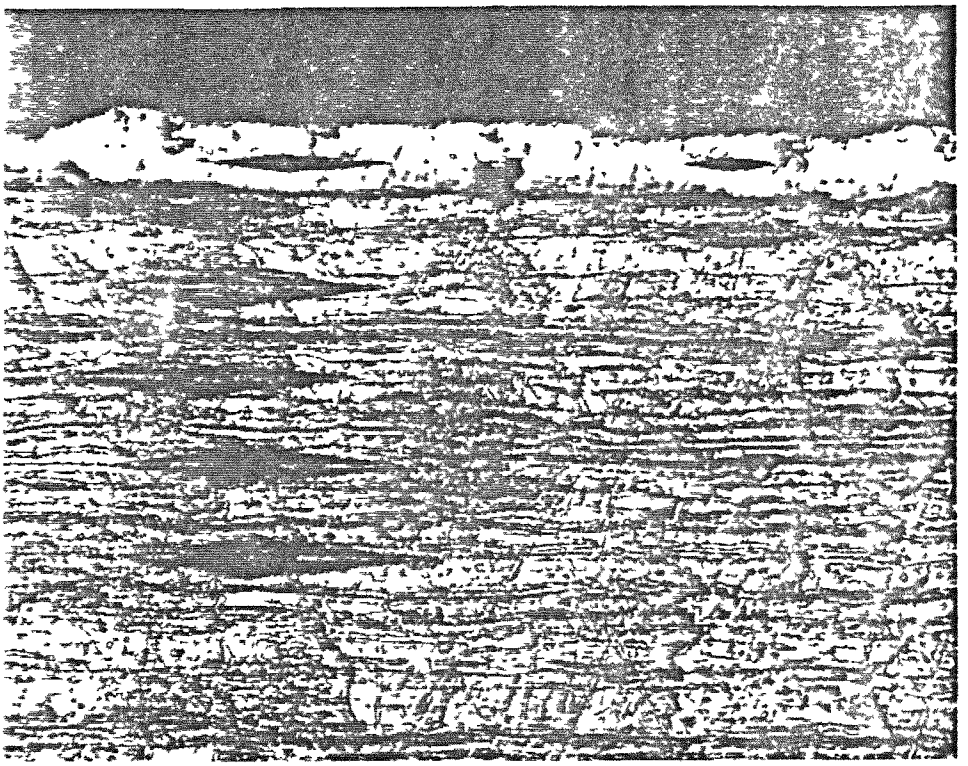

Fig 8.1--Knoop Impressions On a Sectioned Substrate

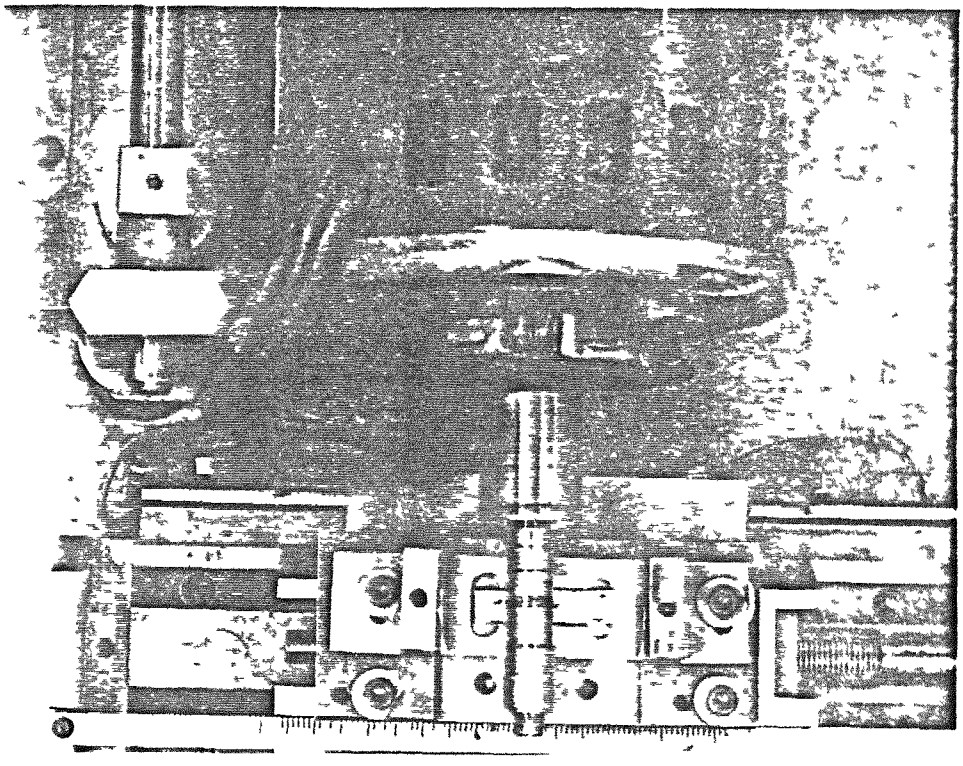

Fig 8.2--Rotary Cylinder Tester

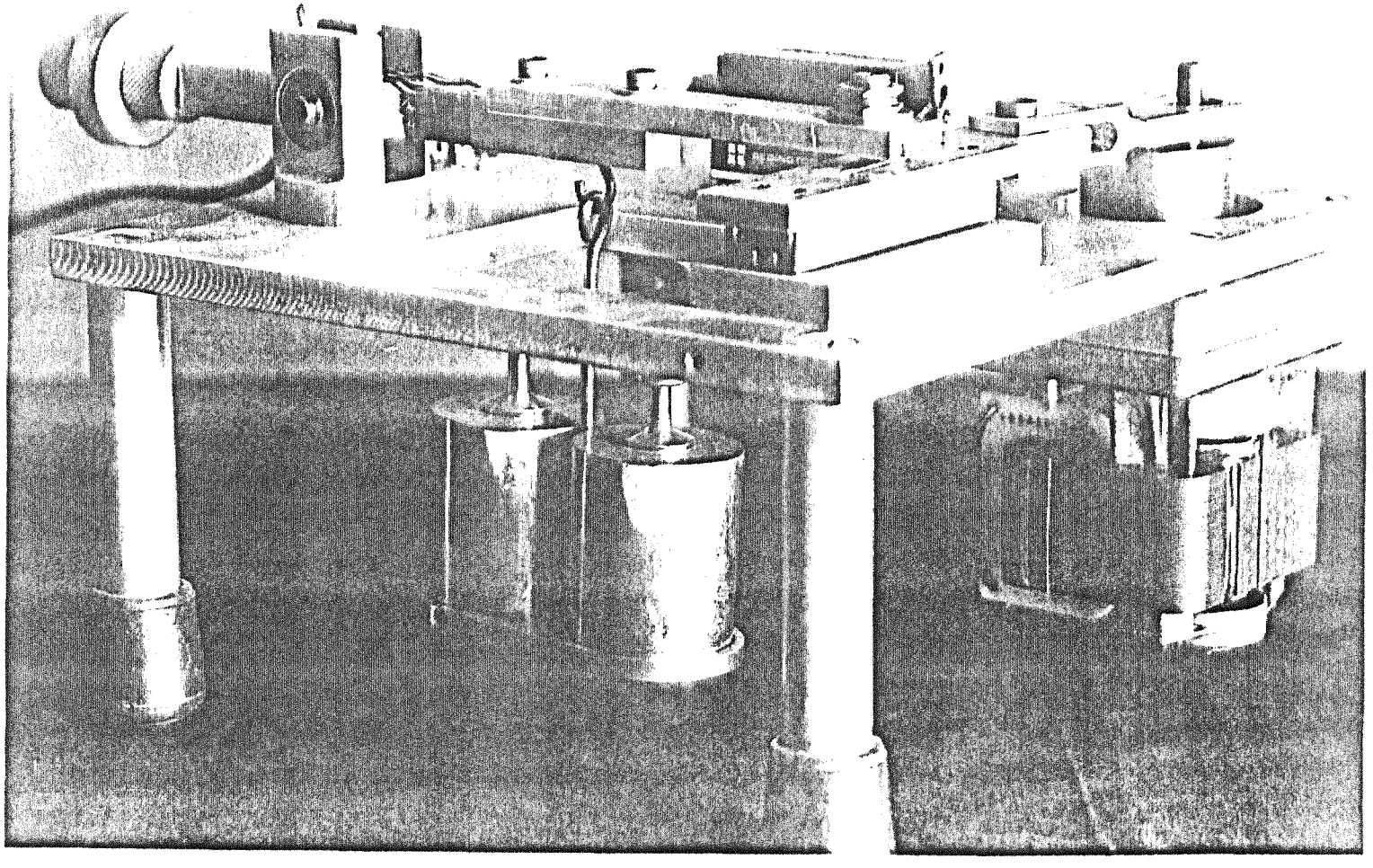

Fig 8.3--Linear Reciprocating Ball Tester

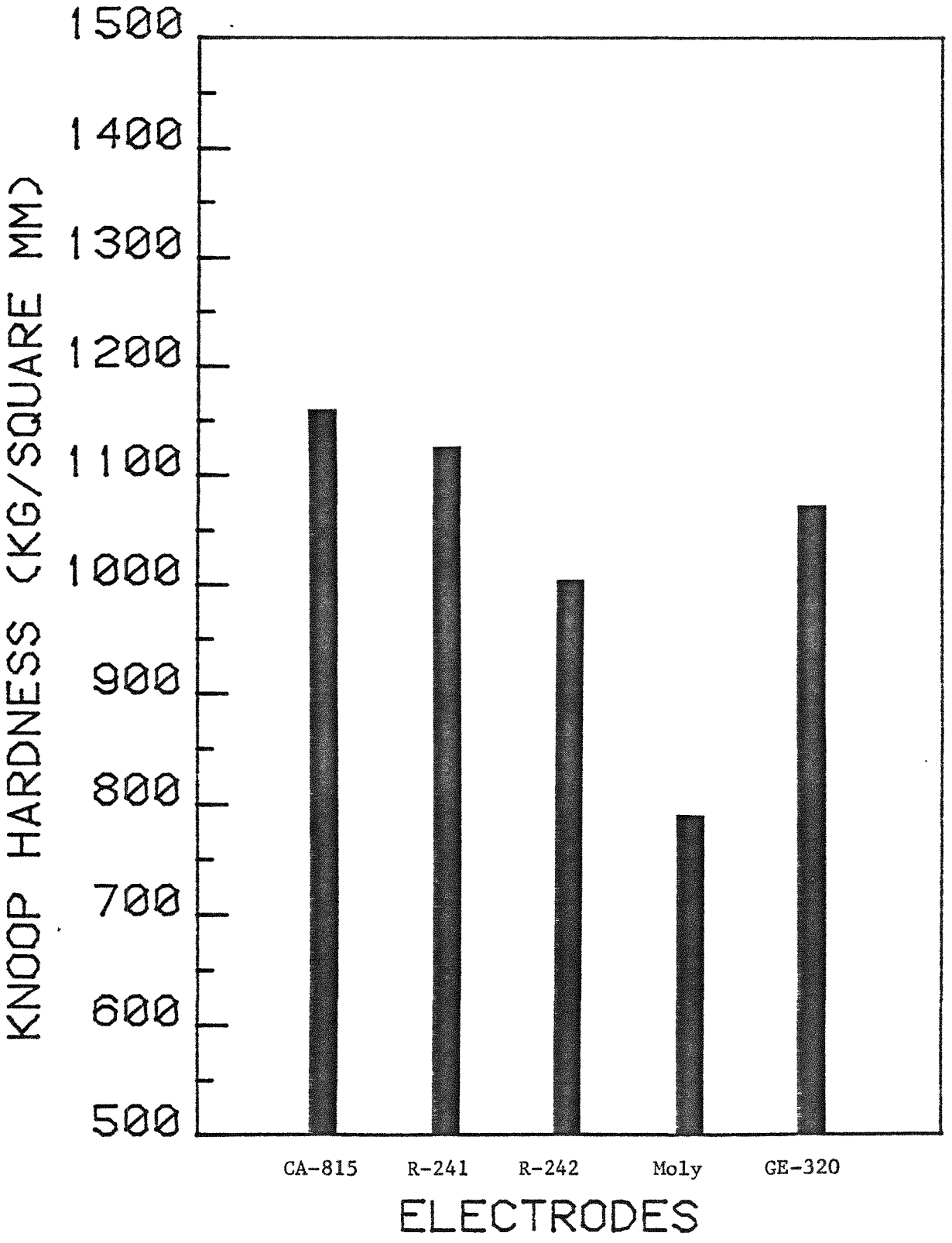

Fig 8.4--Knoop Hardness of Sectioned Coatings

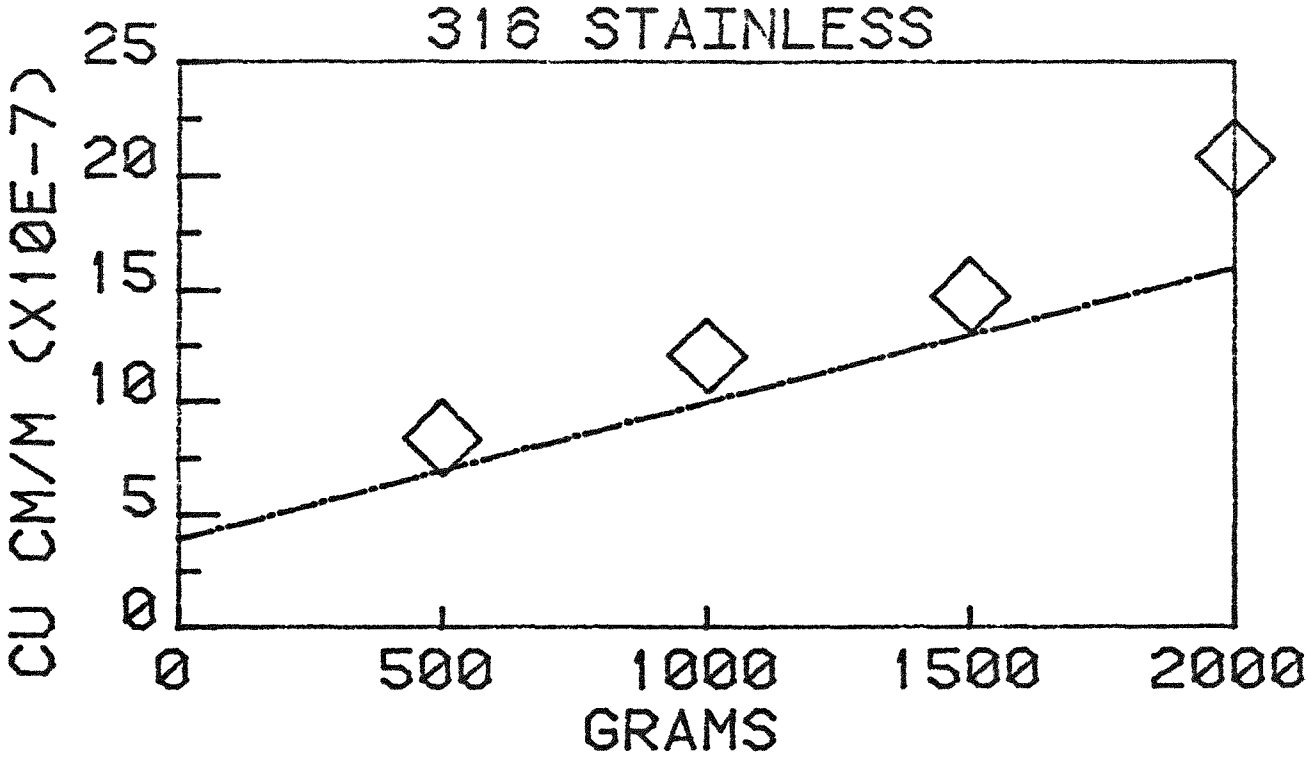

Fig 8.5--Wear Load Curve For Uncoated 316 Stainless Steel Using the Rotary Cylinder Tester

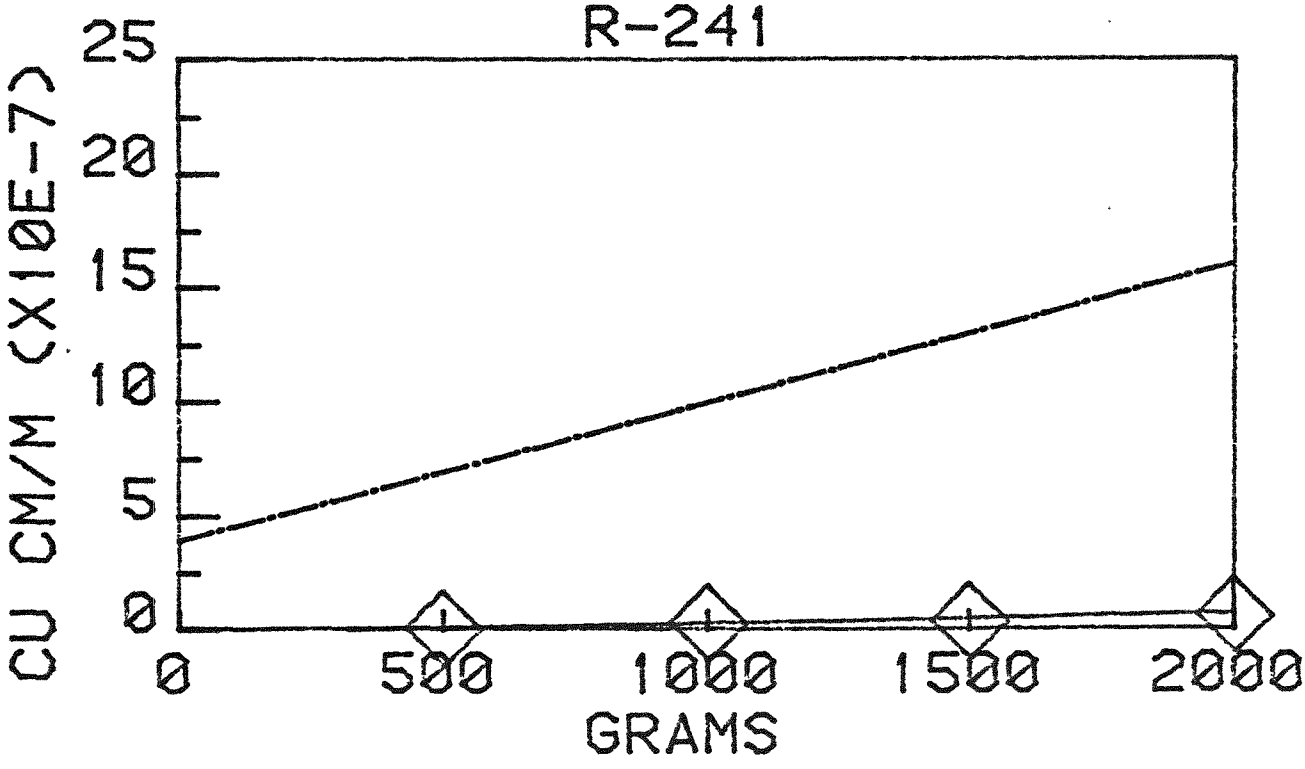

Fig 8.6--Wear Load Curve For R-241 Using the Rotary Cylinder Tester

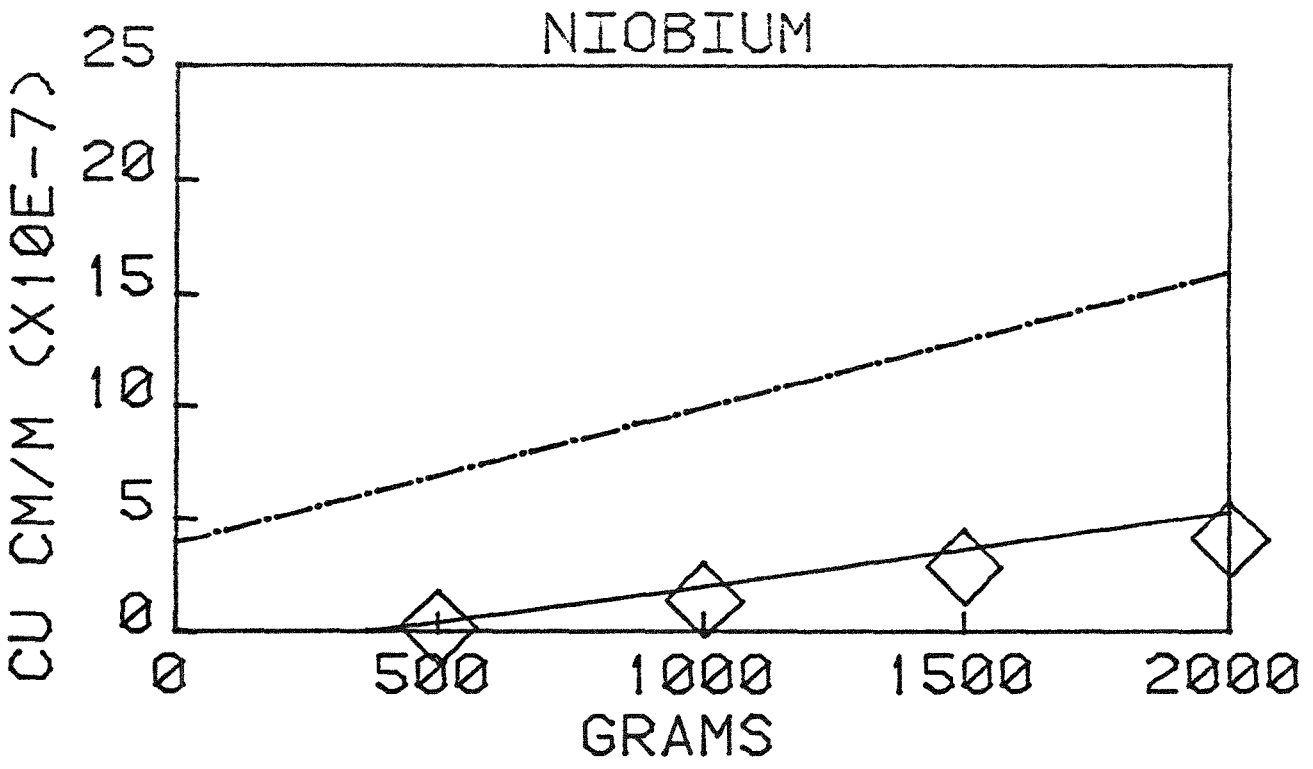

Fig 8.7--Wear Load Curve For Niobium Using the Rotary Cylinder Tester

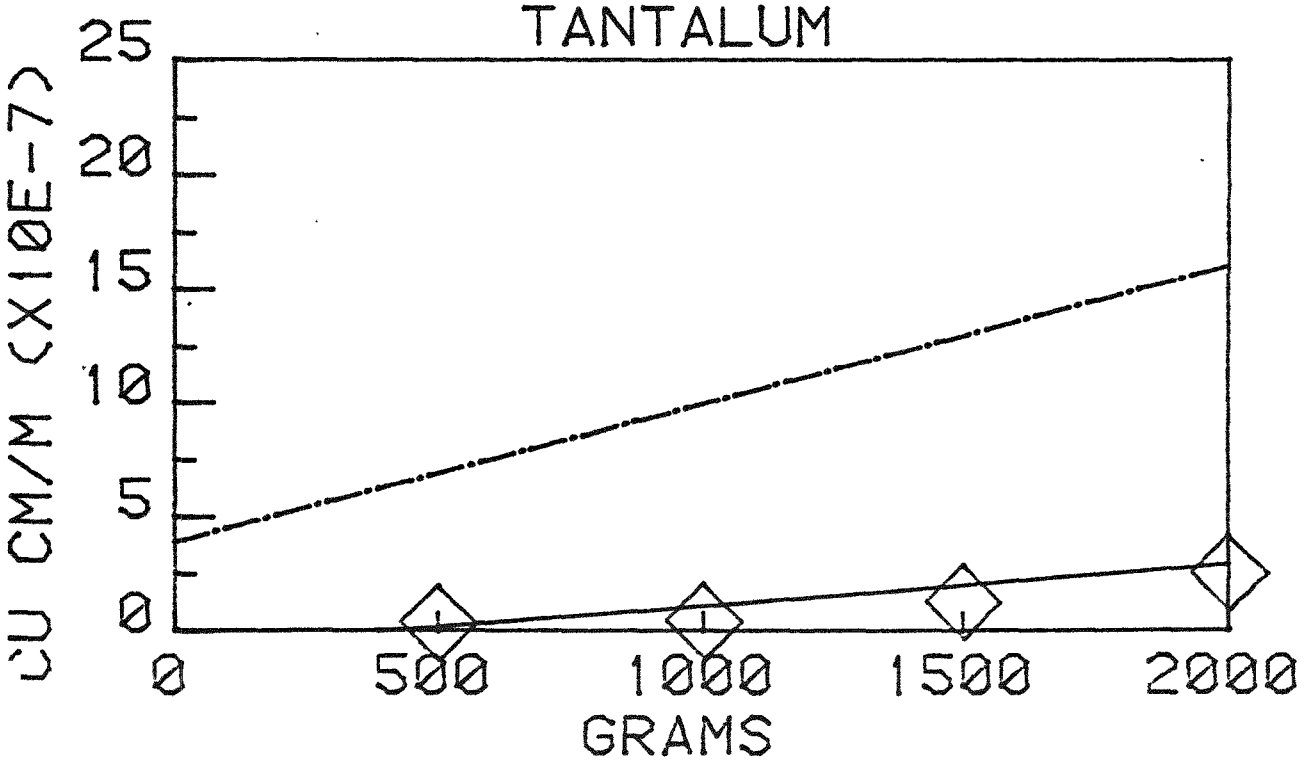

Fig 8.8--Wear Load Curve For Tantalum Using the Rotary Cylinder Tester

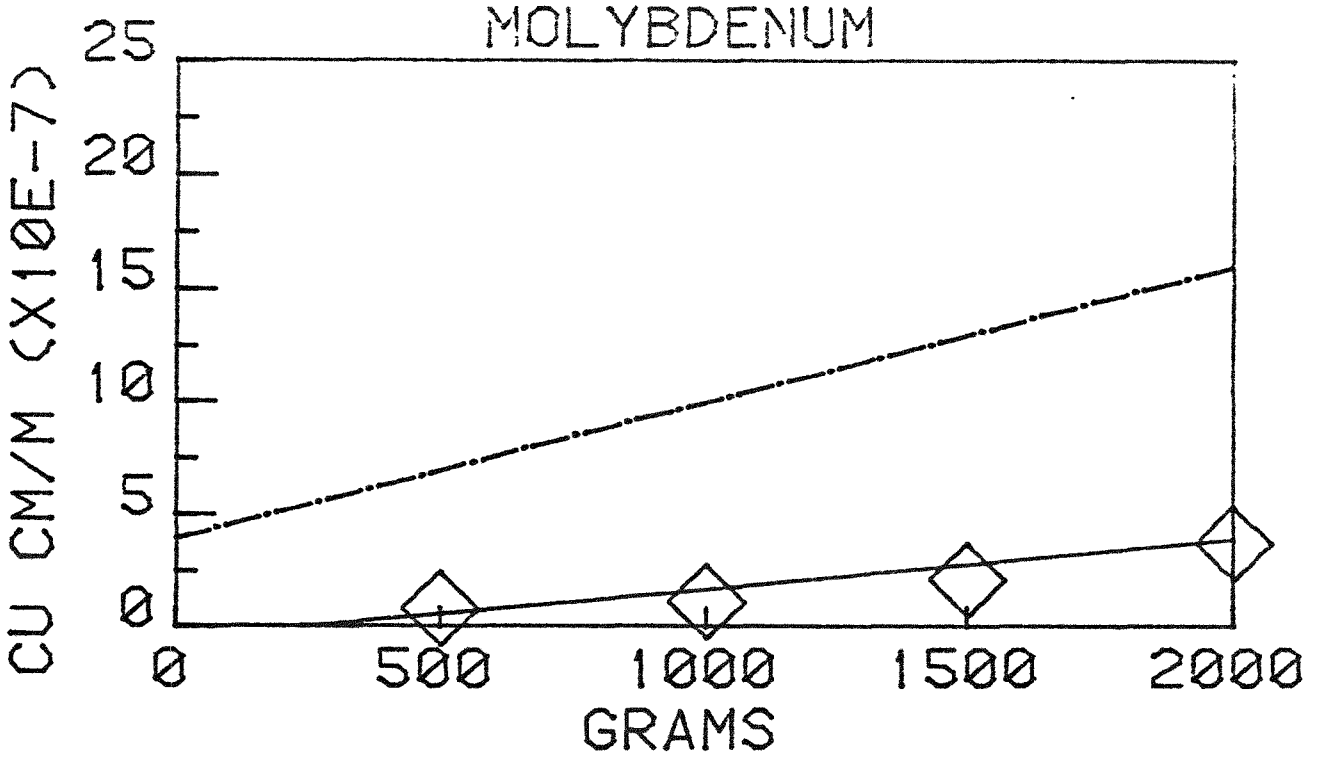

Fig 8.9--Wear Load Curve For Molybdenum Using the Rotary Cylinder Tester

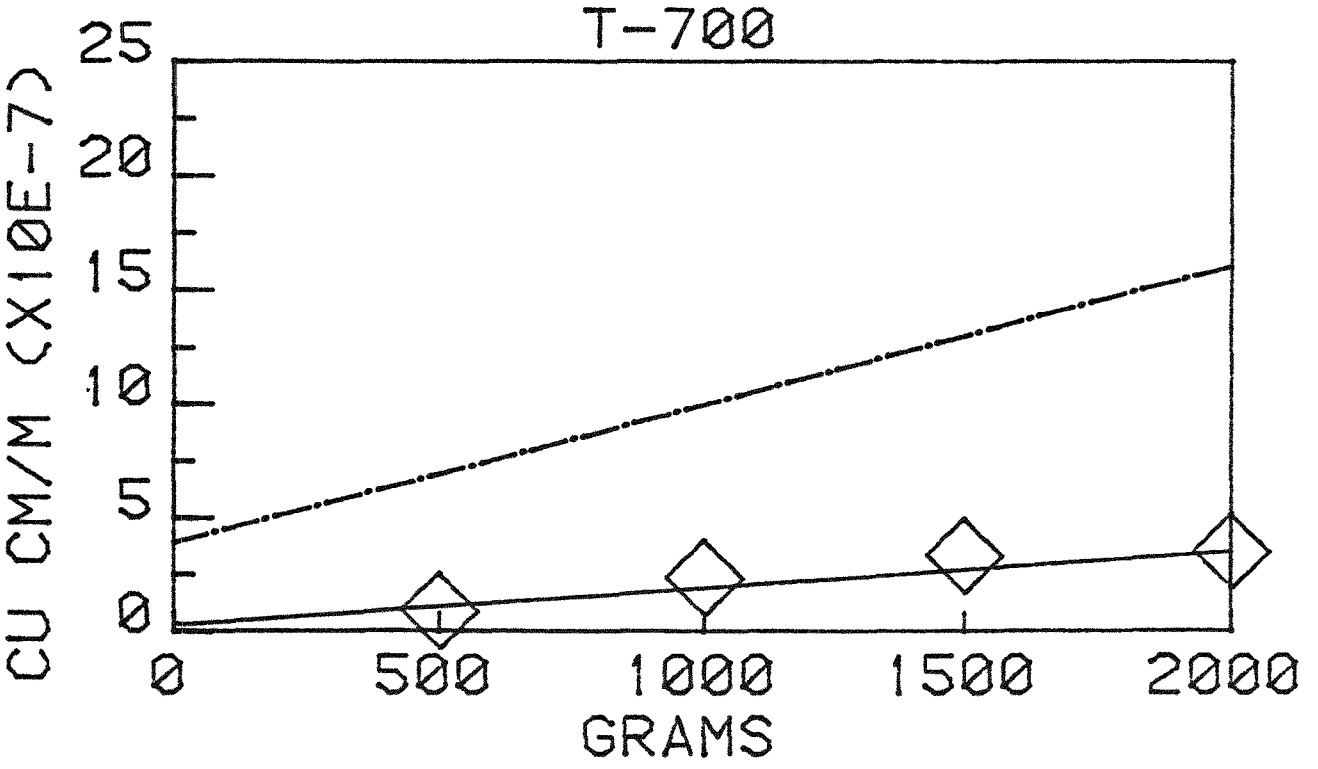

Fig 8.10--Wear Load Curve For T-700 Using the Rotary Cylinder Tester

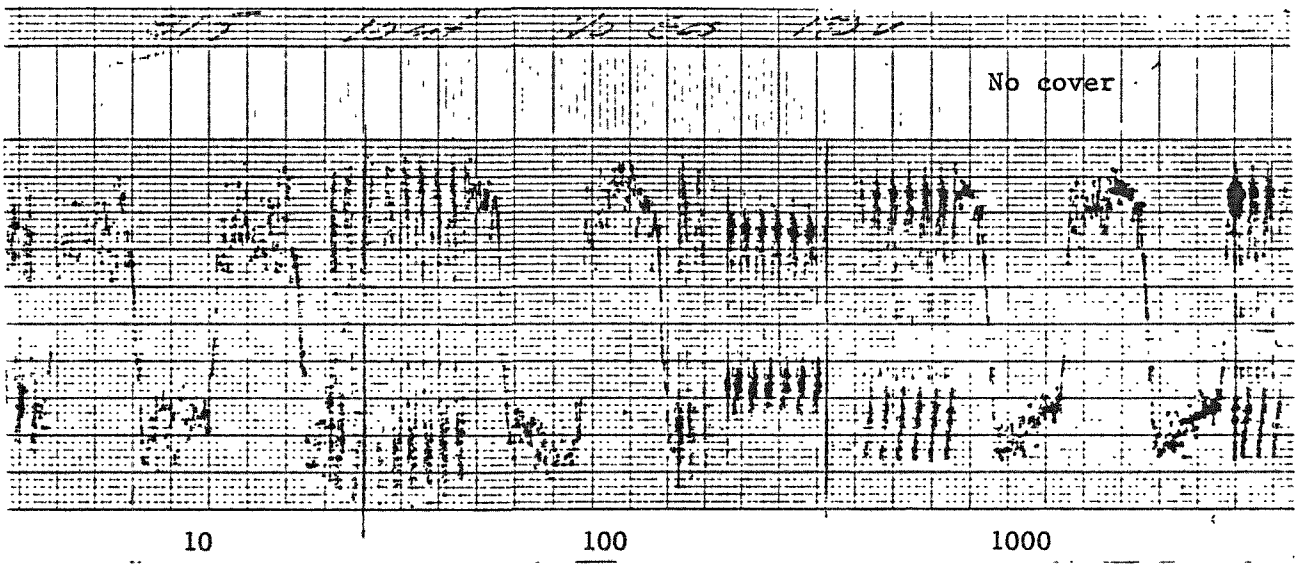

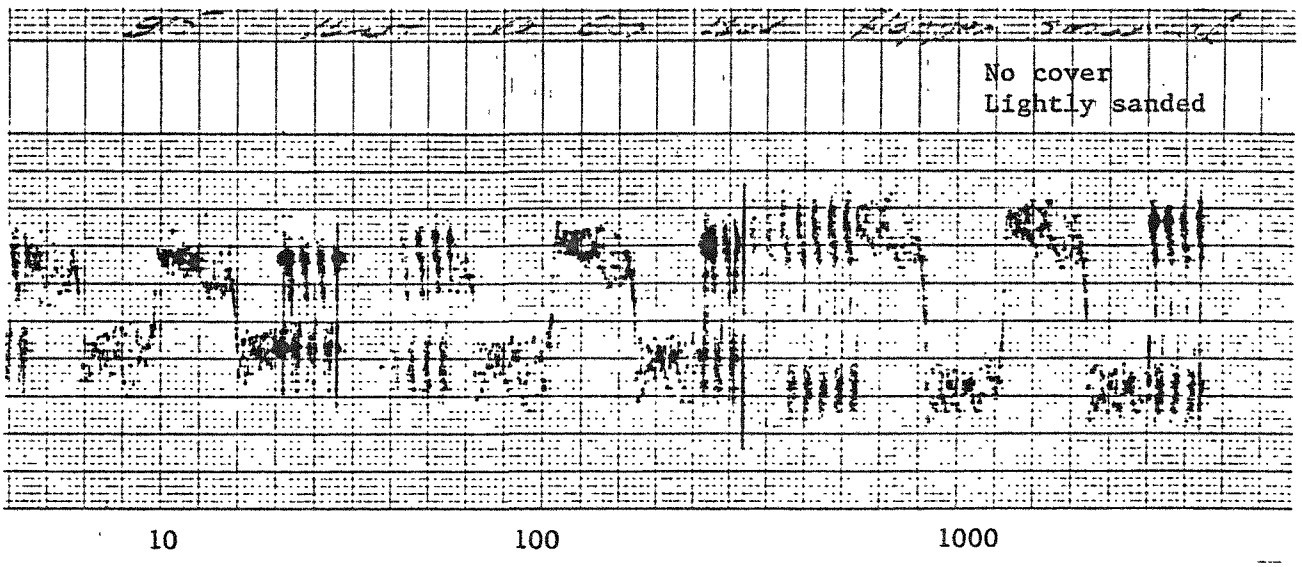

Fig 8.11--Linear Reciprocating Ball Test Trace For CA-815

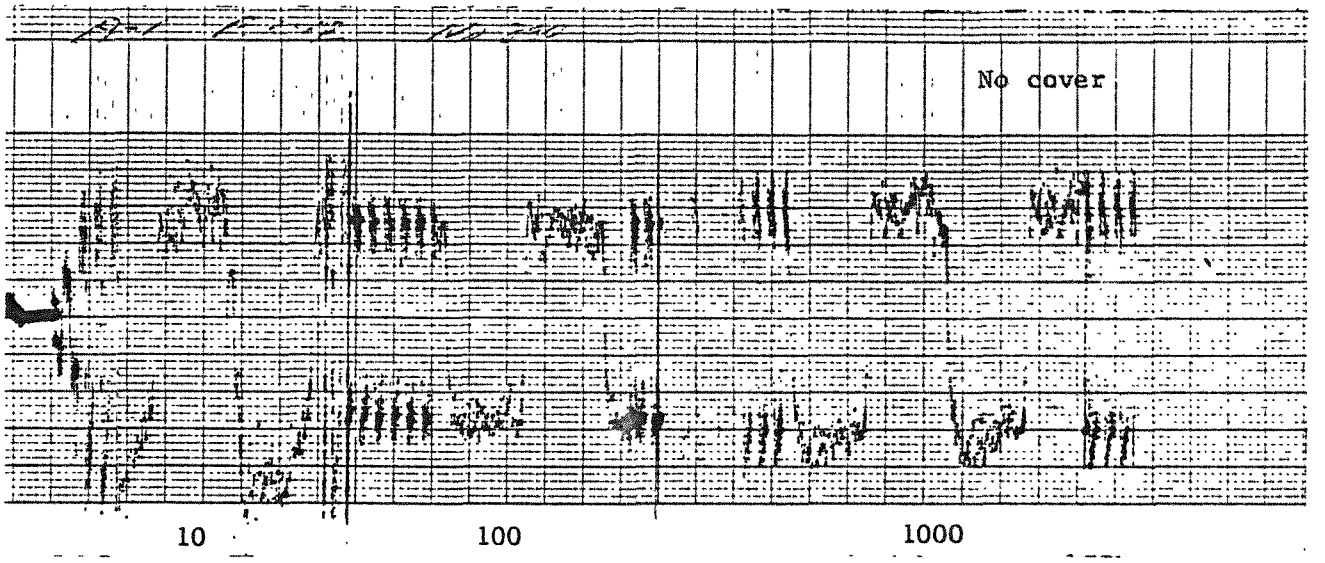

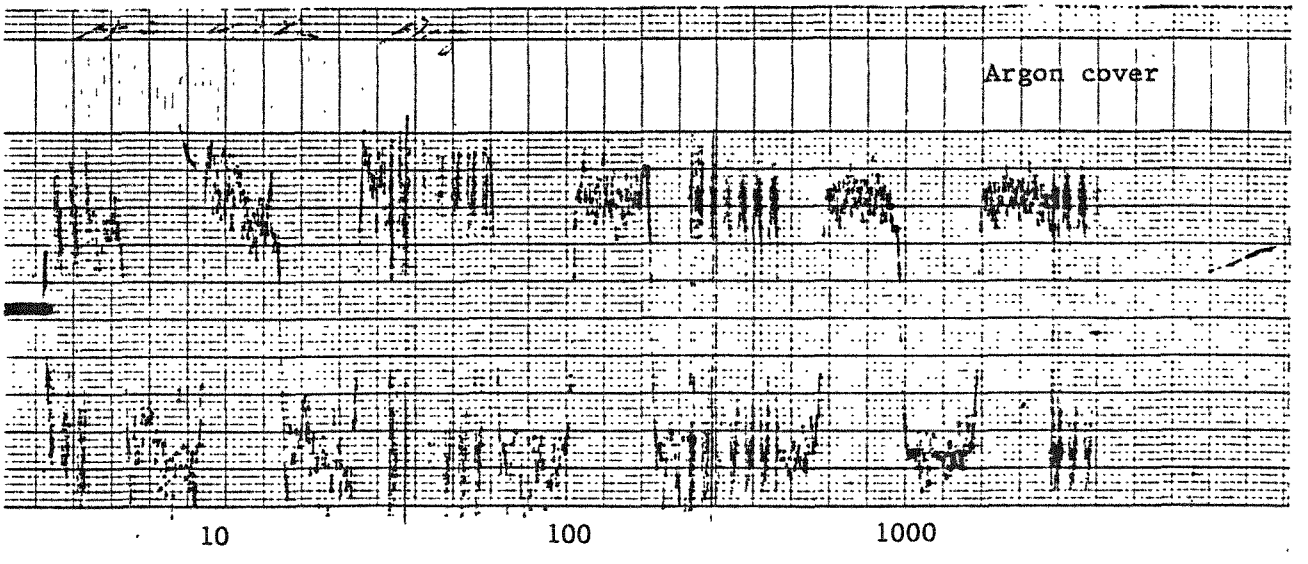

Fig 8.12--Linear Reciprocating Ball Test Trace For R-242

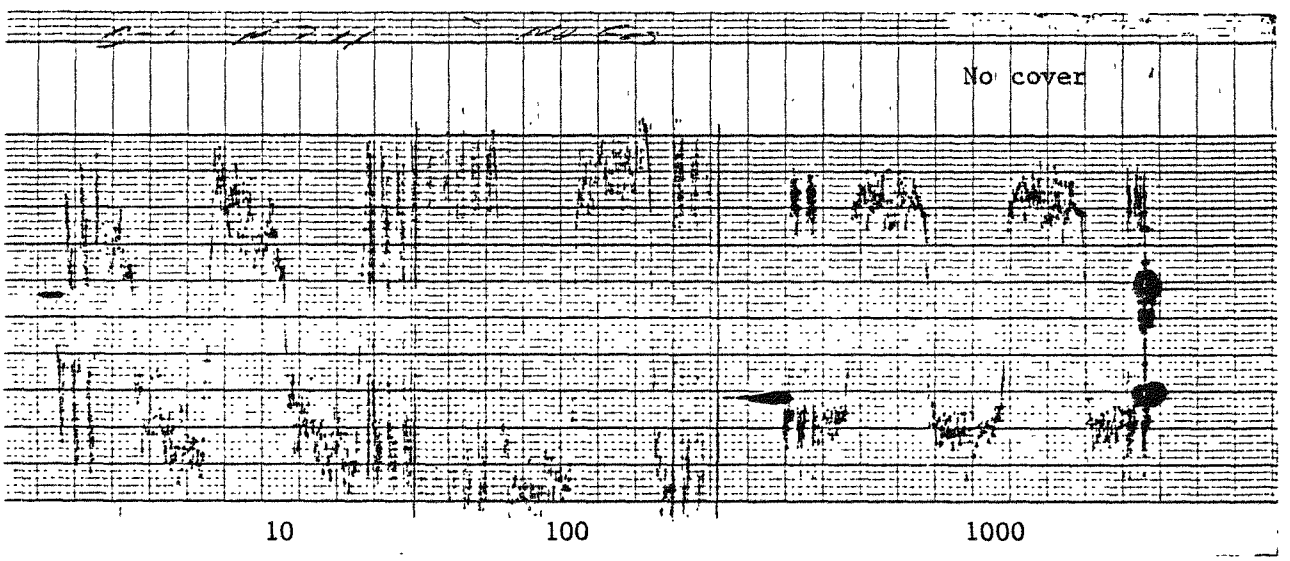

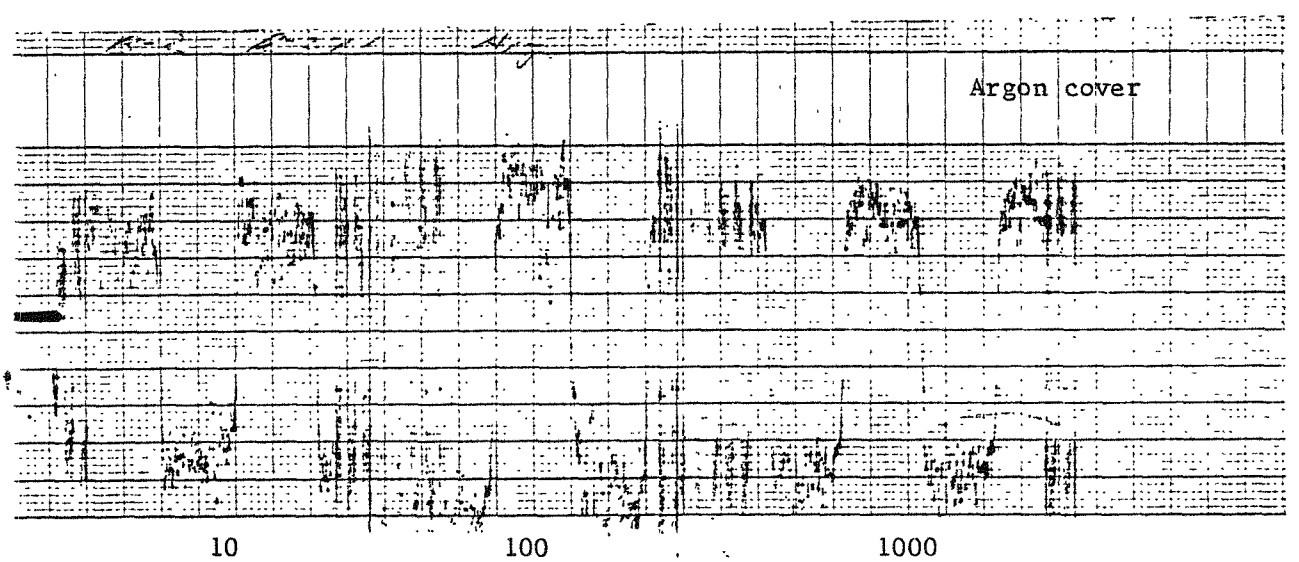

Fig 8.13--Linear Reciprocating Ball Test Trace For R-241

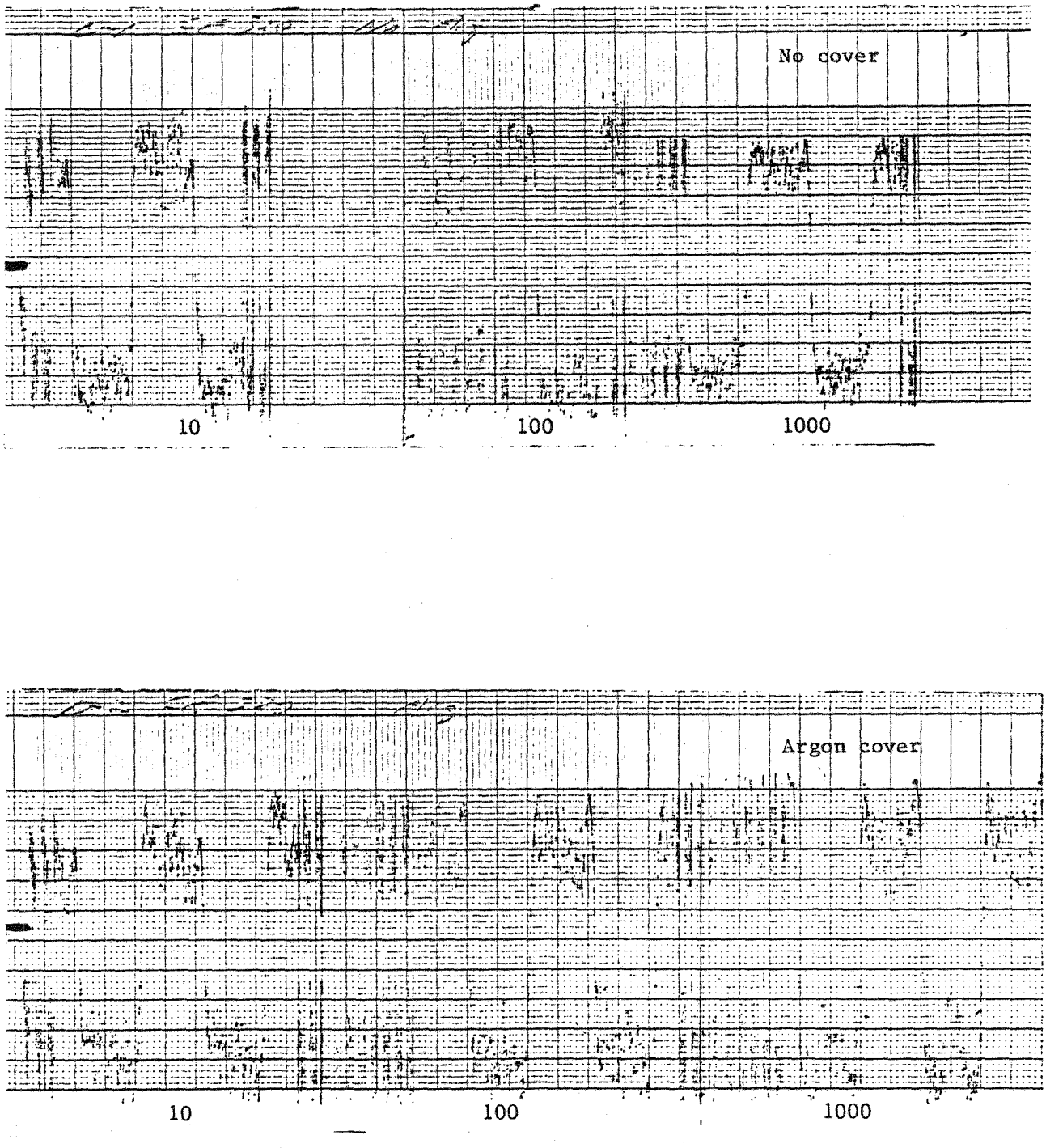

Fig 8.14--Linear Reciprocating Ball Test Trace For GE-320

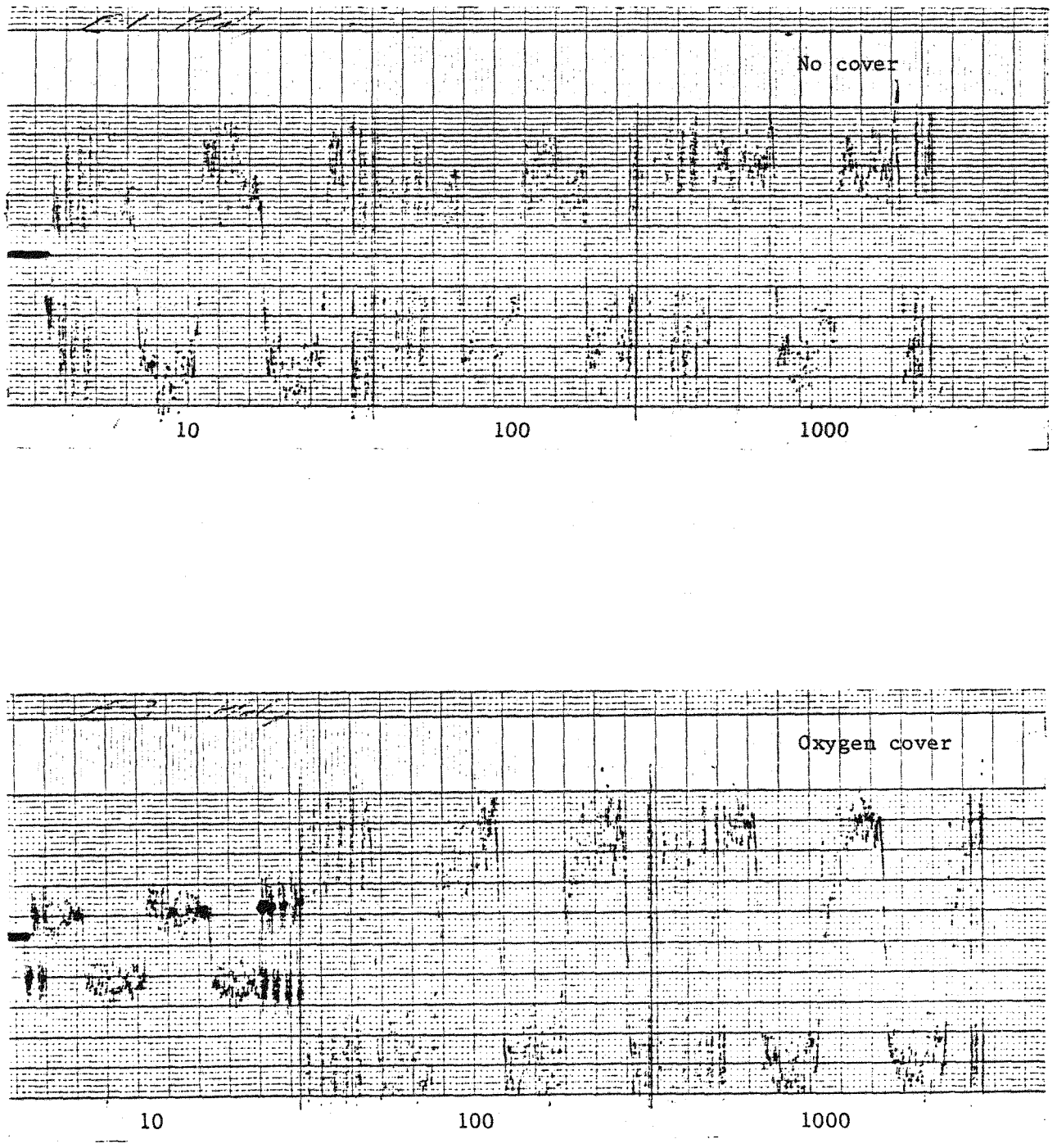

Fig 8.15--Linear Reciprocating Ball Test Trace For Molybdenum

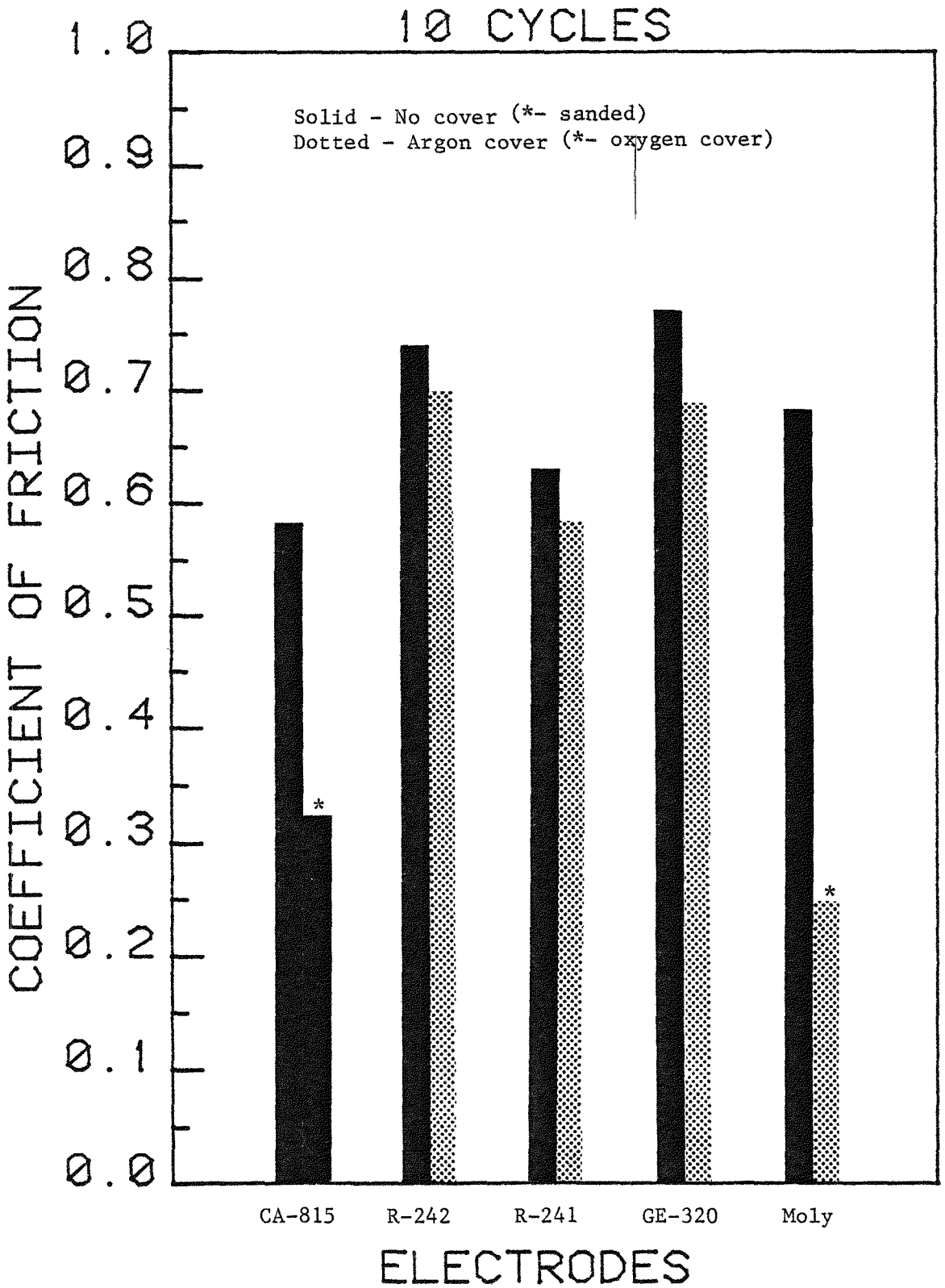

Fig 8.16--Coefficient of Friction for Coatings After 10 Cycles of the Linear Reciprocating Ball Test

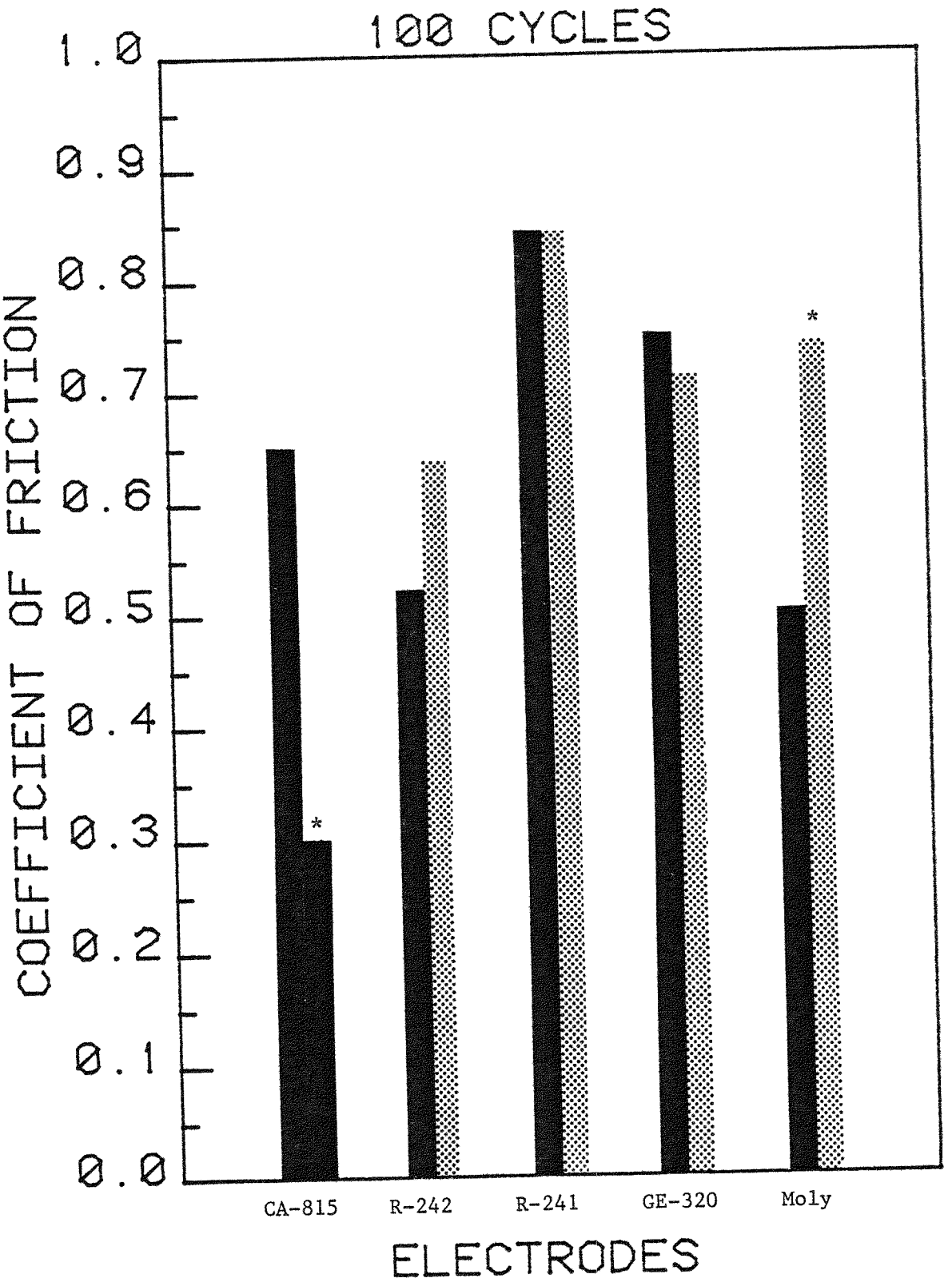

Fig 8.17--Coefficient of Friction for Coatings After 100 Cycles of the Linear Reciprocating Ball Test

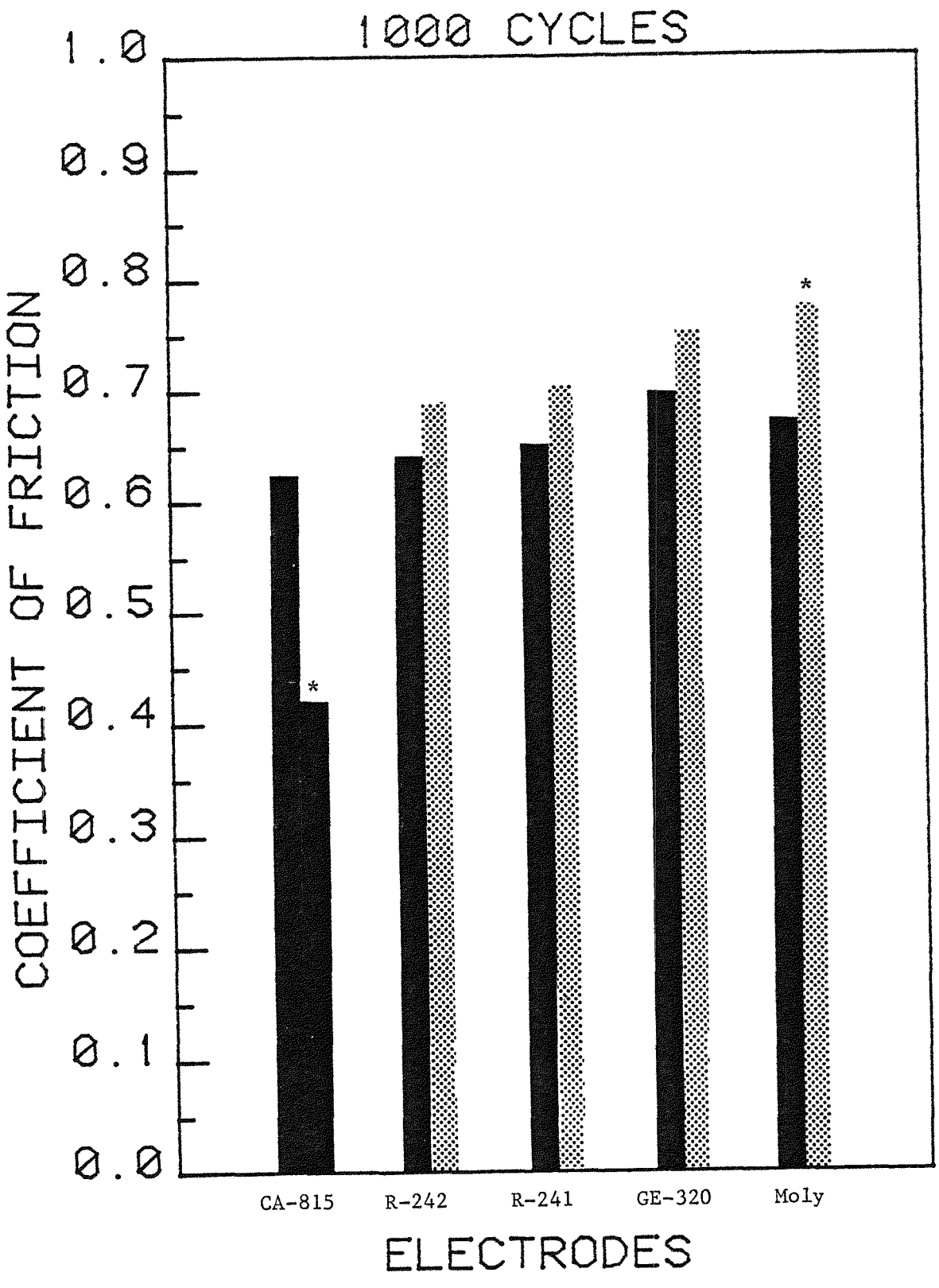

Fig 8.18--Coefficient of Friction for Coatings After 1000 Cycles of the Linear Reciprocating Ball Test

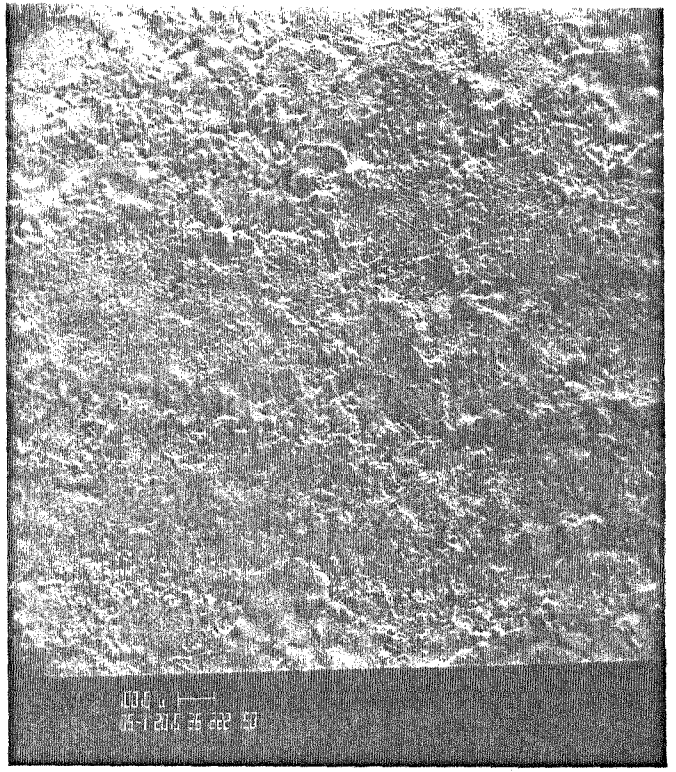

Fig 8.19--SEM Photo of a R-242 Coating Deposited With An Argon Cover Gas

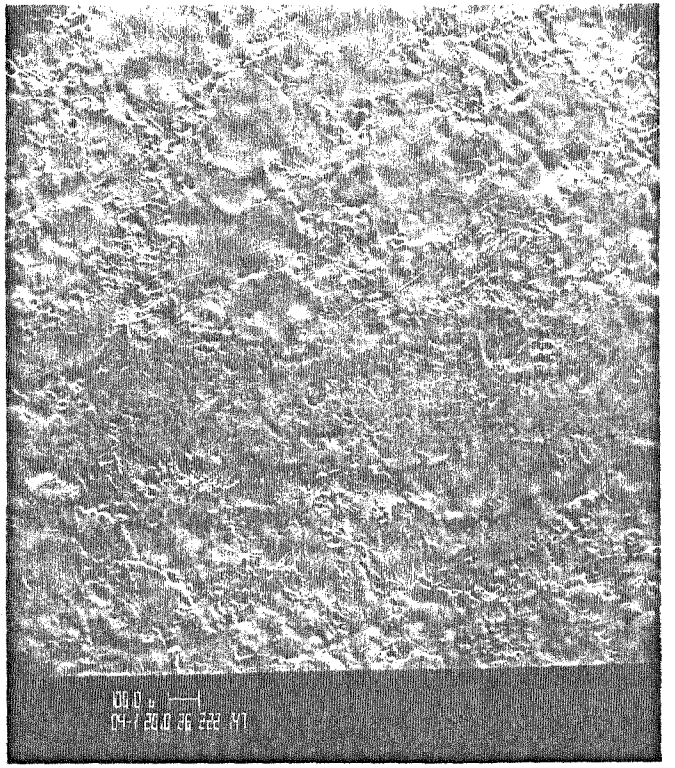

Fig 8.20--SEM Photo of a R-242 Coating Deposited With No Cover Gas

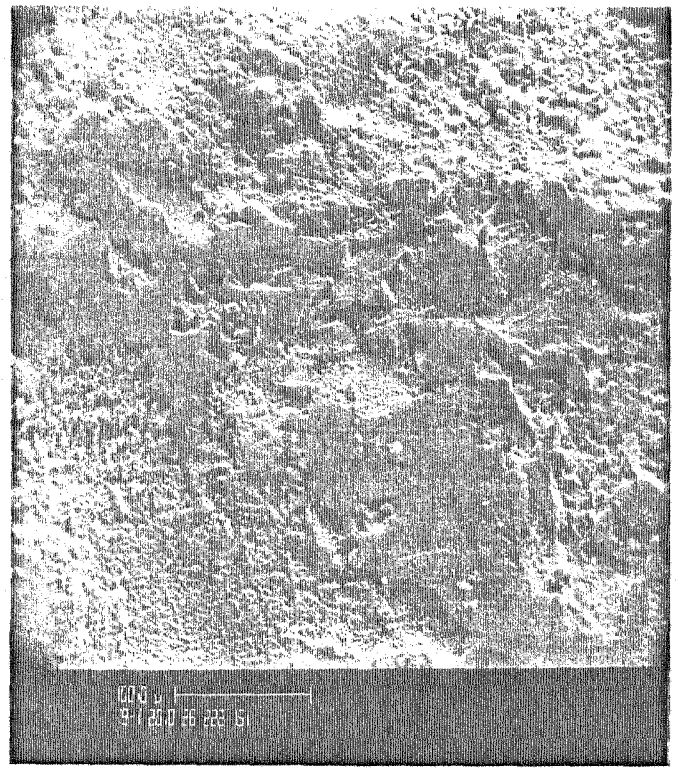

Fig 8.21--SEM Photo of a Linear Reciprocating Ball Wear Track (Fig 8.12) on a R-242 Coating Deposited With an Argon Cover Gas

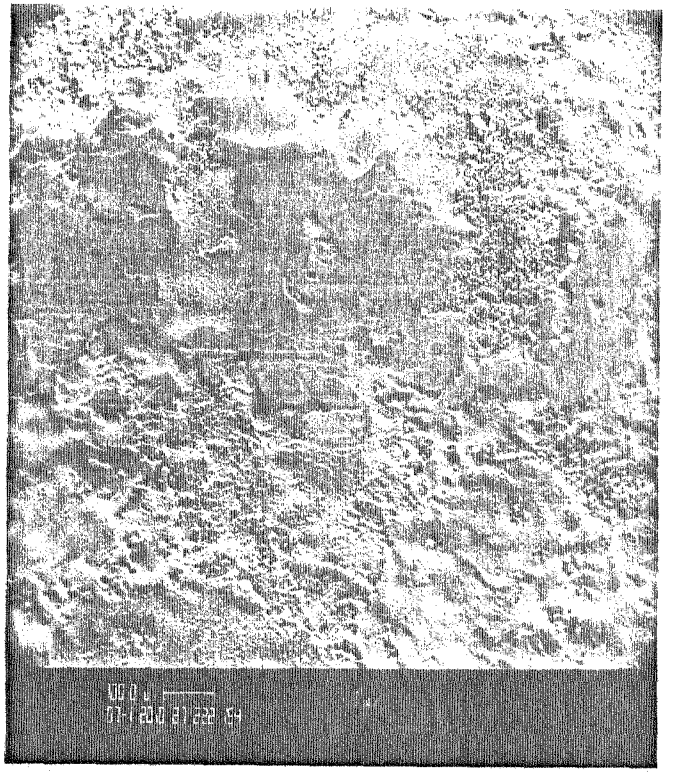

Fig 8.22--SEM Photo of a Linear Reciprocating Ball Wear Track (Fig 8.13) on a R-241 Coating Deposited With an Argon Cover Gas

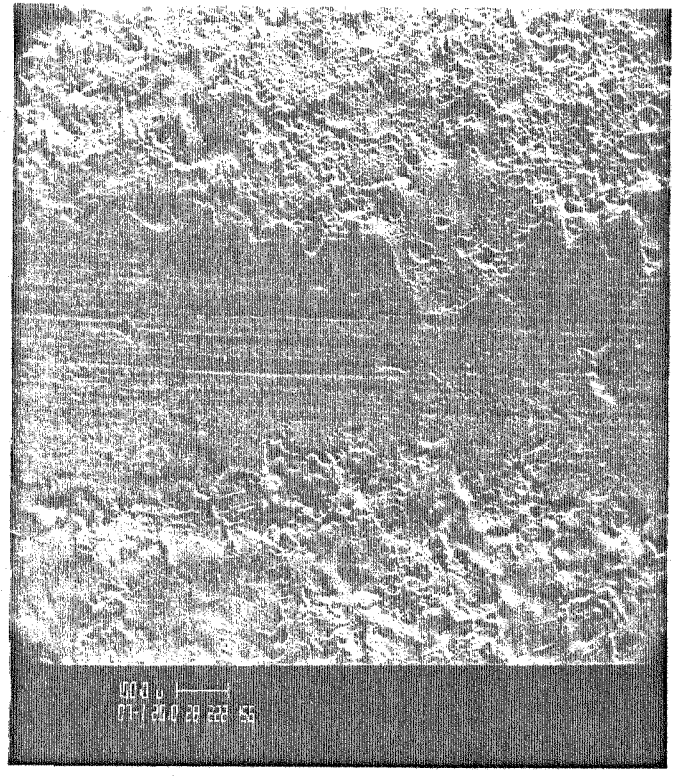

Fig 8.23--SEM Photo of a Linear Reciprocating Ball Wear Track (Fig 8.14) on a GE-320 Coating Deposited With an Argon Cover Gas

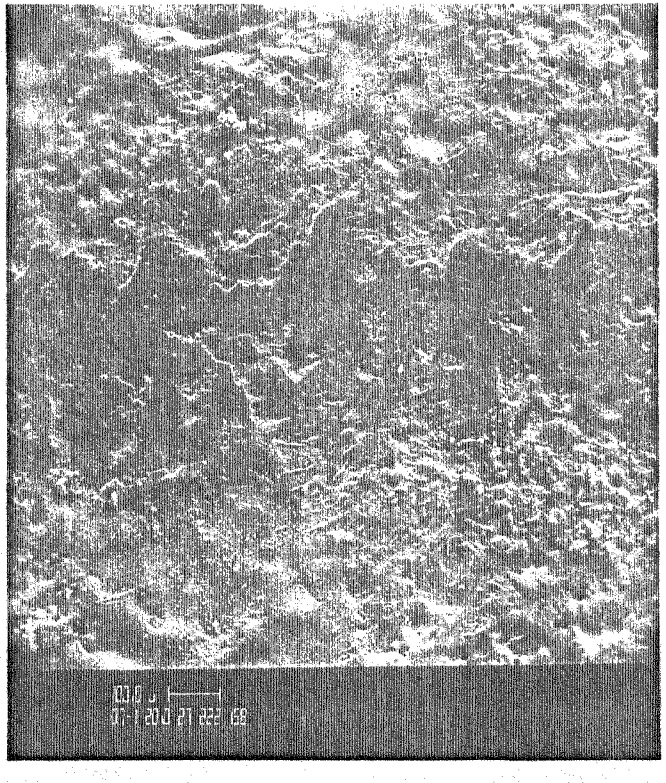

Fig 8.24--SEM Photo of a Linear Reciprocating Ball Wear Track (Fig 8.15) on a Molybdenum Coating Deposited With an Oxygen Cover Gas

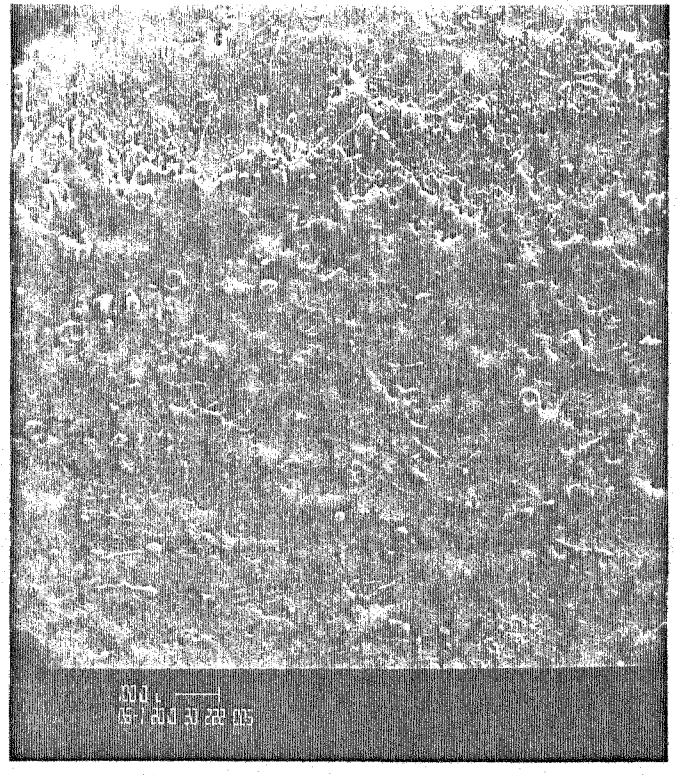

Fig 8.25--SEM Photo of a Linear Reciprocating Ball Wear Track (Fig 8.11) on a CA-815 Coating Deposited With No Cover Gas

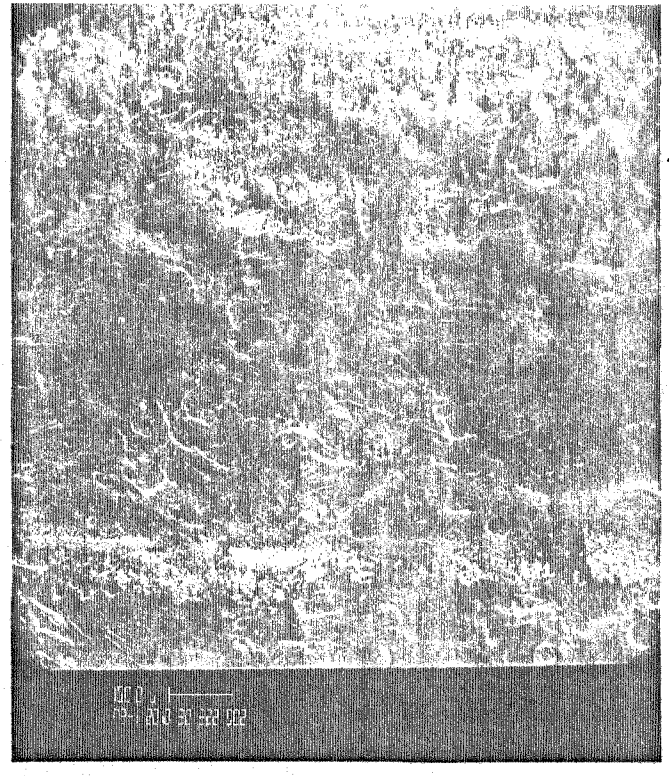

Fig 8.26--SEM Photo of a Linear Reciprocating Ball Wear Track (Fig 8.11) on a CA-815 Lightly Sanded Coating Deposited With No Cover Gas

9 CONCLUSIONS AND RECOMMENDATIONS

After investigating ESD over a period of 20 months, my conclusion is that it is a viable, economical and commercially feasible process for significantly extending the wear life of metals. In light of the recent discovery of using a short duration pulse for controlling lumping, specific recommendations for particular applications may be premature at this time. Up to this point, the best electrode, based on wearability and efficiency is CA-815. The best machine, based on ability to deposit heavily without lumping, is the rotation-oscillation device. However, the electrode data, machine descriptions and operating conditions that have been detailed in this thesis should provide an adequate base on which to design a coating for an intended use.

Testing of the coating for adequacy is an important step in the final selection process. While it is convenient to test coated samples, it may be necessary to test a large finished surface as part of a quality assurance program. Modification to the linear reciprocating ball test apparatus for evaluating larger surfaces would likely be the best choice for a tester, as the information obtained is a real-time record of the coating response and can be used directly with empirical wear equations. Also, damage to the coating is minimal and the testing process is short, reliable and straightforward.

Further research into the ESD process is needed to provide a larger data base from which to draw upon and to give a greater insight into the mechanisms and stoichiometry which occur at the electrode/substrate

interface. New electrode/substrate compositions and their interactions need to be investigated. High production rate, automated applicators will have to be designed to develop ESD into a commercial process. Further refinements in the pulse generation and control circuitry can be made to provide higher reliability and efficiency.

Past and present use of ESD overseas has demonstrated its capabilities in extending the life of metal parts. Hopefully, this thesis will be one step towards bringing Electro-Spark Deposition to its rightful place among the major metal processes of American Industry.

BIBLIOGRAPHY

1 . J.F.Archard, "Wear Theory and Mechanisms", Wear Control Handbook, p 58, 1980

2 . H.S.Rawdon, Trans AIME, Vol. 70, n.37, 1924

3 . N.C.Welsh, "Surface Hardening of Non-Ferrous Metals by Spark Discharge", Nature, Vol.181, p.960, 1957

4 . A.V.Nosov and D.V.Bykov, "Working Metals by Electrosparking", Dept. of Scientific and Industrial Research, HMSO London, 1956

5 . G.P.Ivanov, Stank: Ins, Vol. 22, p.20, 1951

6 . N.C.Welsh and P.E.Watts, "The Wear Resistance of Spark Hardened Surfaces", Wear, Vol.5, 1962

7 . N.C.Welsh, "Spark Hardening of Metals", J. Institute of Metals, Vol. 88, 1956

8 . N.C.Welsh and P.E.Watts, "Spark Hardening of Cutting Tools, Austenitic Formation and Edge Erosion", J. Iron and Steel Inst., p.30, 1961

9 . R.Holm, "Electric Contacts", Almquist and Wiksells, section 40, Stockholm, 1946

10. E.Rabinowicz, "Wear Coefficients-Metals", Wear Control Handbook, p.475, 1980

11. S.P.Fursov, "Some Problems of Finish Spark Alloying", UDC 621.9.048.4, Elektronnaia Obrabotka

12. B.R.Lazarenko, "Electrospark Machining of Metals", Consultants Bureau, Vol 2, 1964

13. A.D.Verkhoturov, "Effect of Pulse Current Frequency on the Formation of a Reinforced Layer in Electro-Spark Alloying", Soviet Powder Metallurgy and Ceramics, Vol 19, n.7, July 1980

14. J.F.Archard, "Contact and Rubbing of Flat Surfaces", Journal of Applied Physics, Vol 24, 1953, pp. 981-988

15. C.S.Kahlon, "Electric Spark Toughening of Cutting Tools and Steel Components", Int.J. Mach. Tool Des. Res., Vol 10, July 1969, pp. 95-121

16. M.M.Barash, C.S.Kahlon, "Experiments With Electric Spark Toughening", Int. J. Mach. Tool Des. Res., Vol 4, 1964, pp.1-8

17. R.F.Bunshah, "Selection and Use of Wear Tests for Coatings", ASTM STP 769, 1981, pp 3-15

18. W.A.Brainard, "Friction and Wear Properties of Three Hard Refractory Coatings Applied By Radiofrequency Sputtering", NASA TN D-8484, May 1977

19. J.F.Lancaster, The Metallurgy of Welding, Brazing and Soldering, Institution of Metallurgists, London, 1970, pp 27-45

20. E.I.Shobert II, "What Happens in EDM", Manufacturing Engineering, July 1976, pp 38-39

21. M.F.Ashby, D.R.H.Jones, Engineering Materials, Pergammon Press, 1980, pp 165, 193-200

22. CRC Handbook of Chemistry and Physics, 53rd edition, 1972

23. C.C.Marty, "Investigation of Surface Temperature in Electro-Discharge Machining", Transactions of the ASME, August 1977, pp 682-684

24. B.Gross, Plasma Technology, American Elsevier Publishing, 1969, pp 215-250

25. O.H.Nestor, "Heat Intensity and Current Density Distribution at the Anode of High Current, Inert Gas Arcs", Physics of the Welding Arc, Inst. of Welding, 1966, pp 50-61

26. L.F.Defize, "Metal Transfer in Gas Shielded Welding Arcs", Physics of the Welding Arc, Inst.of Welding, 1966, pp 112-114